

**Figure 5.** Expression of various 14-3-3 isoforms in reactive astrocytes, surviving oligodendrocytes, and injured axons in chronic demyelinating lesions of MS and in infarcted lesions. The brains of MS and non MS control cases were processed for immunohistochemical analysis using a battery of 14-3-3 isoform-specific antibodies. **a** to **f** represent the following: **a**: No. 609 MS, chronic active demyelinating lesions in the medulla oblongata ( $\gamma$ ). Disrupted axons are stained. **b**: No. 719 acute cerebral infarction, infarcted lesions in the parietal cerebral cortex ( $\epsilon$ ). Reactive astrocytes are stained. **c**: No. 791 MS, chronic inactive lesions in the pons ( $\sigma$ ). Reactive astrocytes are stained. **d**: No. 719 acute cerebral infarction, infarcted lesions in the parietal cerebral cortex ( $\sigma$ ). Reactive astrocytes are stained. **e**: No. 609 MS, chronic active demyelinating lesions in the periventricular white matter of the frontal lobe ( $\theta$ ). Surviving oligodendrocytes are stained. **f**: No. 711 MS, chronic active demyelinating lesions in the optic nerve ( $\theta$ ). Surviving oligodendrocytes are stained.

by incubating the membranes at 50°C for 30 minutes in stripping buffer composed of 62.5 mmol/L Tris-HCl (pH 6.7), 2% SDS, and 100 mmol/L 2-mercaptoethanol, the membranes were processed for relabeling with goat polyclonal antibody against human heat shock protein HSP60 (N-20; Santa Cruz Biotechnology) followed by incubation with horseradish peroxidase-conjugated anti-goat IgG (Santa Cruz Biotechnology). Densitometric analysis was

performed using NIH image version 1.61 software to quantify the intensity of the immunoreactive bands.<sup>36</sup>

#### *Immunoprecipitation Experiments*

To prepare total protein extract for immunoprecipitation experiments, the cells were homogenized in M-PER lysis buffer (Pierce) with a cocktail of protease inhibitors fol-

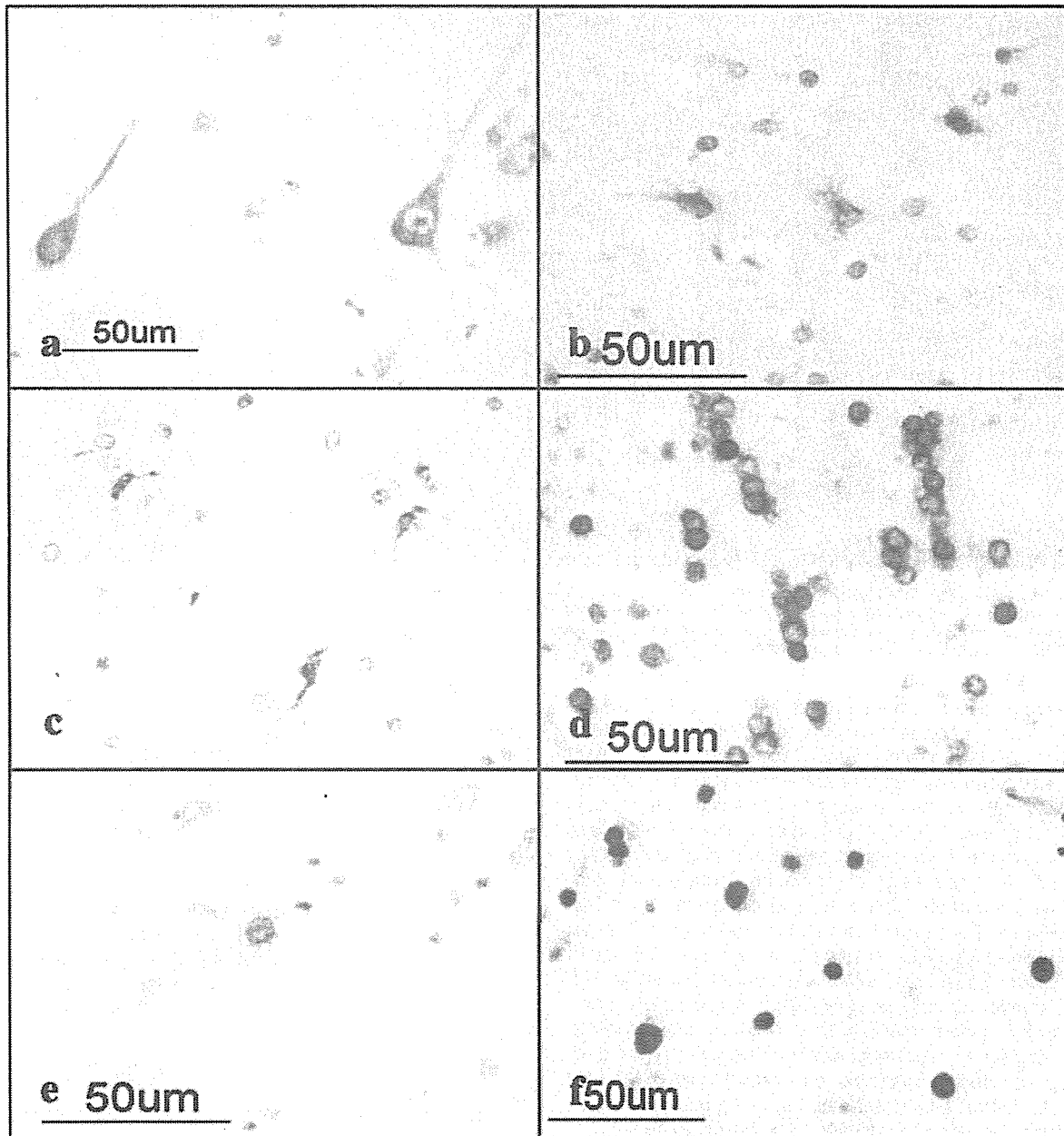


**Figure 6.** Expression of various 14-3-3 isoforms in neurons, astrocytes, oligodendrocytes, and microglia in non-MS brains. The brains of non-MS control cases were processed for immunohistochemical analysis using a battery of 14-3-3 isoform-specific antibodies. a to f represent the following: a: No. G9 neurologically normal subject, the frontal cerebral cortex (3). Cortical neurons are stained. b: No. 523 schizophrenia, frontal cerebral cortex (6). Astrocytes are stained. c: No. 826 schizophrenia, the frontal cerebral cortex (3). Microglia are stained. d: No. 786 acute cerebral infarction, the subcortical white matter of the parietal lobe (1). Surviving oligodendrocytes are stained. e: No. G7 neurologically normal subject, the frontal cerebral cortex (6). A few astrocytes are stained. f: No. 789 old cerebral infarction, the frontal cerebral cortex (1). The nuclei of reactive astrocytes are stained.

lowed by centrifugation at 12,000 rpm at room temperature for 20 minutes. After preclearance, the supernatant was incubated at 4°C for 1 hour with a panel of anti-14-3-3 protein antibodies or the same amount of normal rabbit IgG (Santa Cruz Biotechnology). It was then incubated with Protein G Sepharose (Amersham Bioscience, Piscataway, NJ). After several washes, the immunoprecipitates were processed for Western blot analysis using

V9 antibody or mouse monoclonal antibody against GFAP (GA5; Nichrei).

#### *Two-Dimensional Gel Electrophoresis and Mass Spectrometry Analysis*

To prepare total protein extract for two-dimensional gel electrophoretic analysis, the cells were homogenized in

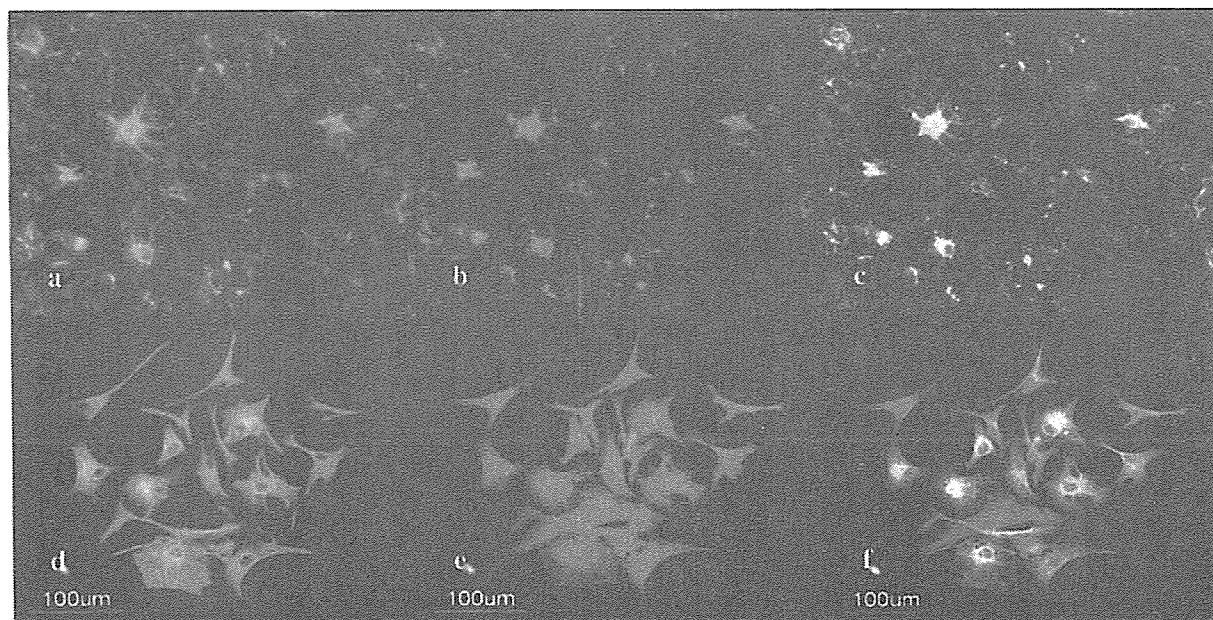


**Figure 7.** Co-expression of the 14-3-3 $\epsilon$  isoform and GFAP in reactive astrocytes in chronic demyelinating lesions of MS and in cultured human astrocytes. Cultured human astrocytes and MS brain tissues were processed for double immunolabeling with anti-GFAP antibody and  $\epsilon$  isoform-specific antibody followed by labeling with fluorescein isothiocyanate- and rhodamine-conjugated secondary antibodies. **a to f** represent no. 741, chronic active demyelinating lesions in the subcortical white matter of the frontal lobe (**a-c**), cultured human astrocytes (AS-BW) (**d-f**). GFAP (**a, d**),  $\epsilon$  (**b, e**), and the overlay (**c, f**).

rehydration buffer composed of 8 mol/L urea, 2% CHAPS, 0.5% carrier ampholytes (pH 4 to 6), 20 mmol/L dithiothreitol, 0.002% bromophenol blue, and a cocktail of protease inhibitors and phosphatase inhibitors (Sigma). Urea-soluble protein was separated by isoelectric focusing using the ZOOM IPGRunner system (Invitrogen) loaded with an immobilized pH 4.5 to 5.5 gradient strip. After the first dimension of isoelectric focusing, the protein was separated in the second dimension on a NuPAGE 4 to 12% polyacrylamide gel (Invitrogen). The gel was stained using Coomassie brilliant blue G-250 solution or the Silverquest silver staining kit (Invitrogen). It was transferred onto a polyvinylidene difluoride membrane for protein overlay and Western blot analysis. Spots of interest were excised from the gels, trypsinized, and processed for mass spectrometry (nanoESI-MS/MS) analysis followed by database searching using MASCOT software (Invitrogen Proteome, Yokohama, Japan).

### Protein Overlay Analysis

To prepare the 14-3-3 protein-specific probe for protein overlay analysis, the open reading frame of the human 14-3-3 $\epsilon$  isoform gene (YWHAE, GenBank accession No. NM\_006761) was amplified from the cDNA of Ntera2-N cells by the polymerase chain reaction using sense and anti-sense primers (5'atggatgatcgagaggatctggtg3' and 5'tcactgatttctgcttccacgctc3'). The polymerase chain reaction product was cloned into a prokaryotic expression vector pTrcHis-TOPO (Invitrogen). The expression of recombinant human 14-3-3 $\epsilon$  protein having an N-terminal Xpress tag for detection (rh14-3-3 $\epsilon$ ) was induced in *Escherichia coli* by exposure to isopropyl  $\beta$ -thiogalactoside. The recombinant protein was further purified through a

HiTrap chelating HP column (Amersham Bioscience) and by separation on a 12% SDS-PAGE gel. Recombinant human interferon-stimulated protein ISG15 fused to an N-terminal Xpress tag (rhISG15), a vimentin-binding protein in human cancer cells,<sup>37</sup> was prepared for the control probe. The polyvinylidene difluoride membrane on which the gel was blotted was incubated at room temperature overnight with 1  $\mu$ g/ml rh14-3-3 $\epsilon$  or rhISG15 probe, followed by immunolabeling with mouse monoclonal anti-Xpress antibody (Invitrogen) and horseradish peroxidase-conjugated anti-mouse IgG. After the probes and antibodies were stripped by incubating the membrane at 50°C for 30 minutes in stripping buffer, it was repeatedly relabeled with V9 antibody, GA5 antibody, or rabbit polyclonal antibodies specific for phosphorylated Ser-39, Ser-72, or Ser-83 epitopes of vimentin (Santa Cruz Biotechnology), followed by incubation with horseradish peroxidase-conjugated anti-mouse or rabbit IgG.

### Results

#### Growth-Dependent Expression of 14-3-3 Isoforms in Cultured Human Astrocytes

To investigate the expression pattern of seven 14-3-3 isoforms in human neural cells, cultured human astrocytes, Ntera2-N neurons, and U-373MG astrocytoma cells, all of which were incubated in 10% FBS-containing culture medium, were processed for Western blot analysis using a panel of isoform-specific antibodies or the antibodies broadly reactive against all of the isoforms listed in Table 1. Cultured human astrocytes, neurons, and astrocytoma cells, along with

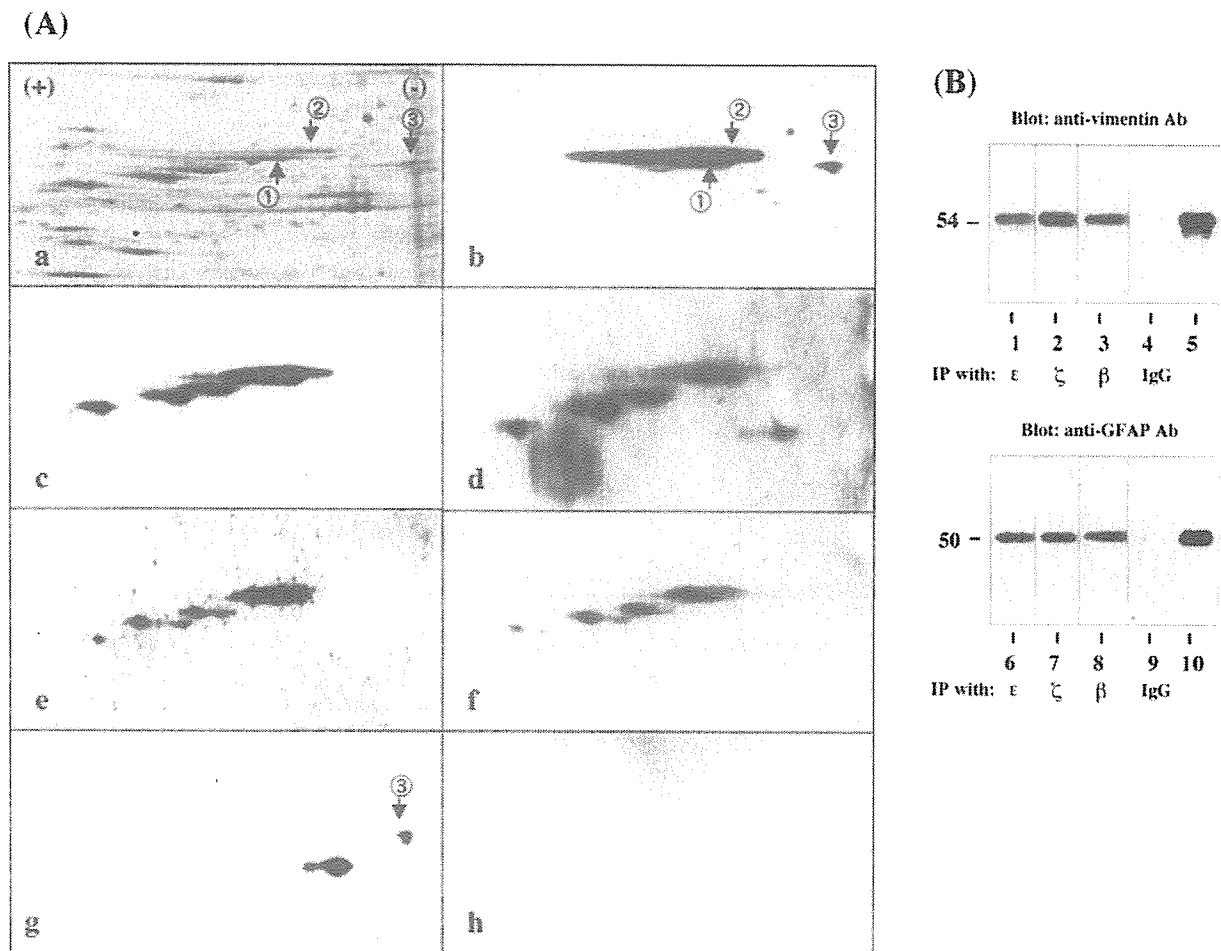


**Figure 8.** Two-dimensional gel electrophoresis and immunoprecipitation analysis of 14-3-3  $\epsilon$  isoform-binding proteins in cultured human astrocytes. **A:** Two-dimensional gel analysis. Human astrocytes (AS-BW) were incubated in 10% FBS-containing culture medium. Twenty-one  $\mu$ g of total protein extract was separated on a two-dimensional PAGE gel, transferred onto a polyvinylidene difluoride membrane, and processed for overlay analysis with recombinant human 14-3-3 $\epsilon$  protein possessing the Xpress tag (rh14-3-3 $\epsilon$ ) followed by labeling with anti-Xpress antibody. After the probe and antibody were stripped, the blot was repeatedly relabeled six times with the antibodies against GFAP, vimentin, and vimentin with specific phosphorylated serine epitopes, and with recombinant human interferon-stimulated protein ISG15 having the Xpress tag (rhISG15). **a** to **g** represent silver staining (a), rh14-3-3 $\epsilon$  labeling followed by staining with anti-Xpress antibody (b), vimentin (c), vimentin with phosphorylated Ser-59 (d), vimentin with phosphorylated Ser-72 (e), vimentin with phosphorylated Ser-83 (f), GFAP (g), and rhISG15 labeling followed by staining with anti-Xpress antibody (h). Two major spots labeled with rh14-3-3 $\epsilon$  and anti vimentin antibody are named spot no. 1 and no. 2, while a spot labeled with rh14-3-3 $\epsilon$  and anti-GFAP antibody is designated spot no. 3. Spots no. 1 and no. 2 were excised from the gel and processed for mass spectrometry (MS) analysis. **B:** Immunoprecipitation analysis. Total protein extract of cultured human astrocytes was immunoprecipitated with  $\epsilon$  isoform-specific antibody (lanes 1 and 6),  $\zeta$  isoform-specific antibody (lanes 2 and 7),  $\beta$  isoform-specific antibody (lanes 3 and 8), with the same amount of normal rabbit IgG (lanes 4 and 9), or untreated with any antibodies (lanes 5 and 10; 2  $\mu$ g of total protein extract before processing for immunoprecipitation). Then, the immunoprecipitates were processed for Western blot analysis using anti vimentin (top) or anti-GFAP antibody (bottom).

human brain homogenate, expressed substantial levels of  $\beta$ ,  $\gamma$ ,  $\epsilon$ ,  $\zeta$ ,  $\eta$ , and  $\theta$  isoforms (Figure 1, a to h; lanes 1 to 4). In contrast, the  $\sigma$  isoform was undetectable in human neural cells but was identified in HeLa cells (Figure 1i, lanes 1 to 5).

To study the effects of culture conditions on 14-3-3 protein levels, human astrocytes were incubated for 7 days in 10% FBS-containing culture medium or in the serum-free culture medium, which led to nearly complete growth arrest. The expression levels of  $\beta$ ,  $\gamma$ ,  $\epsilon$ ,  $\zeta$ ,  $\eta$ , and  $\theta$  isoforms were elevated in human astrocytes incubated in the serum-containing growth-promoting condition. The expression was enhanced 3.3-, 1.6-, 2.2-, 10.0-, 18.7-, or 4.6-fold, respectively, compared

with the levels under the serum-free growth-arrested condition when standardized against the levels of HSP60, a housekeeping gene product on the identical blots (Figure 2, a to c, e to g; top and bottom panels, lanes 1 and 2). The serum-induced up-regulation of 14-3-3 isoforms was also observed in a different culture of human astrocytes (Figure 2d, top and bottom panels, lanes 1 and 2) and mouse astrocytes in culture (Figure 2h, top and bottom panels, lanes 1 and 2; and additional data shown in Supplementary Figure 2 on The American Journal of Pathology website at <http://www.amjpathol.org>). These results indicate that cultured human astrocytes constitutively express all iso-

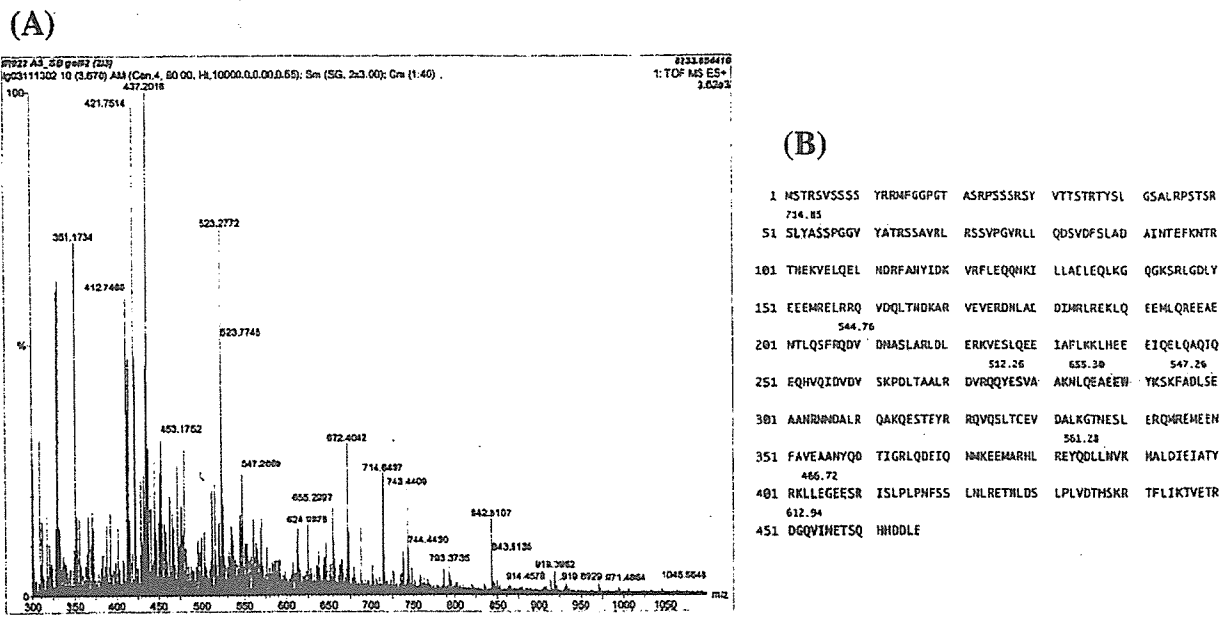


**Figure 9.** Mass spectrometry analysis of the 14-3-3 $\epsilon$  isoform-binding proteins in cultured human astrocytes. Spots no. 1 and no. 2 labeled with the rh14-3-3 $\epsilon$  probe (Figure 5A, a and b) were excised from the gel, trypsinized, and processed for nanoESI-MS MS analysis. **A:** The spectra of nanoESI-MS MS analysis of spot no. 1. Each peak indicates individual peptide fragments. The position of several peaks was automatically numbered on the spectra. Peptides derived from the autolytic fragments of trypsin (eg. 112, 121, and 523) were omitted to be processed for further analysis. The peptide fragments were selected for MS analysis in order of their signal intensity. **B:** Amino acid sequence of human vimentin. Eight peptide fragments of spot no. 1 identified by nanoESI-MS MS analysis (shadowed) showed a perfect match with the amino acid sequence encompassing residues 51 to 466 of vimentin. The number indicated on each fragment represents the position in the horizontal axis of the spectra (A).

forms except for  $\sigma$ , whose levels were elevated in a cell growth-dependent manner.

### Differential Expression of 14-3-3 Isoforms in Reactive Astrocytes in Demyelinating Lesions of MS

To investigate the differential expression of seven 14-3-3 isoforms in MS lesions, the brain, spinal cord; and optic nerve of four progressive MS patients (no. 791, no. 744, no. 609, and no. 544) and 12 non-MS control cases were processed for immunohistochemistry using a panel of isoform-specific antibodies. In chronic active and inactive demyelinating lesions of MS, the majority of GFAP<sup>+</sup> hypertrophic astrocytes intensely expressed  $\beta$ ,  $\epsilon$ ,  $\zeta$ , and  $\eta$  isoforms, whereas a small population of reactive astrocytes displayed immunoreactivities against  $\gamma$ ,  $\theta$ , and  $\sigma$  isoforms (Table 2; Figure 3, a to e; Figure 4 a and b). Reactive astrocytes immunoreactive against the 14-3-3 protein exhibited the most dense accumulation at the lesion edge, although they were widely distributed in demyelinating lesions and in the normal appearing white matter. A glial scar was also intensely labeled with the antibodies against  $\beta$ ,  $\epsilon$ ,  $\zeta$ , and  $\eta$  isoforms ( $\epsilon$  shown in Figure 3e and the others not shown). In MS and non-MS brains, a major population of cerebral cortical neurons constitutively expressed high levels of  $\beta$ ,  $\gamma$ ,  $\zeta$ , and  $\eta$  isoforms, and to a lesser degree,  $\theta$  isoform, whereas they hardly showed immunoreactivity for the  $\sigma$  isoform, and a small population of cerebral cortical neurons in MS and non-MS brains occasionally expressed weak immunore-

activity for the  $\epsilon$  isoform, although these findings varied among brains for different cases (Table 2; Figure 4, c to f; and Figure 6). Disrupted, distorted, and swollen axons found in the active demyelinating lesions of MS exhibited strong immunoreactivity against  $\gamma$  and  $\zeta$  isoforms ( $\gamma$  shown in Figure 5a and the other not shown).

A very small population of reactive astrocytes in demyelinating lesions of MS, which occasionally showed a binucleated morphology, intensely expressed the  $\sigma$  isoform, whose expression was not detected in cultured human astrocytes (Figure 5c). A number of reactive astrocytes that appeared in the ischemic lesions of cerebral infarction expressed strong immunoreactivity against  $\epsilon$ ,  $\zeta$ , and  $\eta$  isoforms (Table 2; Figure 5b), and the  $\sigma$  isoform was again strongly expressed in a very small number of reactive astrocytes (Figure 5d). The immunoreactivity against the  $\eta$  isoform was often concentrated in the nuclear region of reactive astrocytes in MS lesions (not shown) and the ischemic lesions (Figure 6: a to f). Furthermore, some GFAP<sup>+</sup> astrocytes occasionally identified in the brains of schizophrenia and neurologically normal patients expressed  $\epsilon$  and  $\sigma$  isoforms at variable levels (Table 2; Figure 6, b and e). CD68<sup>+</sup> macrophages and microglia, with the greatest accumulation identified in the center and edge of active demyelinating lesions of MS and necrotic lesions of cerebral infarction, expressed  $\beta$ ,  $\zeta$ , and  $\eta$  isoforms, whereas they did not show substantial immunoreactivity against  $\epsilon$ ,  $\theta$ , or  $\sigma$  isoforms (Table 2; Figure 6c). CD3<sup>+</sup> lymphocytes found in the perivascular cuffs of active MS lesions expressed variable immunoreactivities for  $\beta$  and  $\zeta$  isoforms (not shown). A substantial

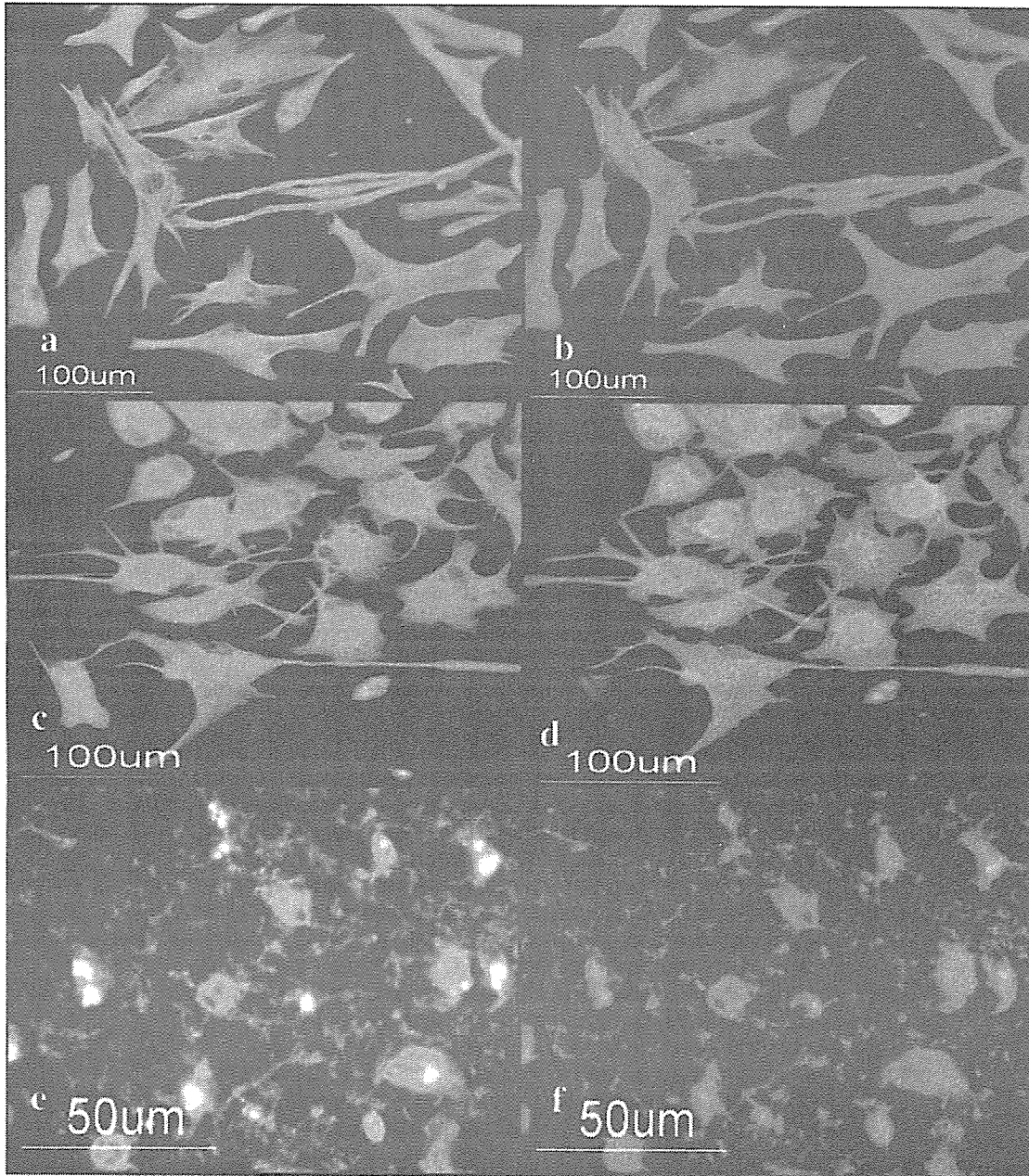


**Figure 10.** Co-expression of the 14-3-3  $\epsilon$  isoform and vimentin in cultured human astrocytes and reactive astrocytes in chronic demyelinating lesions of MS. Cultured human astrocytes and MS brain tissues were processed for double immunolabeling with anti-vimentin antibody and  $\epsilon$  isoform-specific antibody or anti-GFAP antibody followed by labeling with fluorescein isothiocyanate- and rhodamine-conjugated secondary antibodies. **a** to **f** represent cultured human astrocytes (AS-BW) (**a-d**); no. 71, chronic active demyelinating lesions in the subcortical white matter of the frontal lobe (**e, f**): vimentin (**a, c, e**);  $\epsilon$  (**b, f**); and GFAP (**d**).

population of oligodendrocytes, which survived in chronic active demyelinating lesions of MS and ischemic lesions of cerebral infarction, expressed intense immunoreactivity against  $\theta$  isoform (Table 2; Figure 5, e and f; and Figure 6d). These results suggest that markedly up-regulated expression of the  $\epsilon$  isoform is the most reliable marker for identifying reactive astrocytes in MS and non-MS brains. Co-expression of the  $\epsilon$  isoform and GFAP was verified in reactive astrocytes in MS lesions

(Figure 7; a to c) and cultured human astrocytes (Figure 7; d to f) by double immunolabeling.

#### *Binding of the 14-3-3 $\epsilon$ Isoform to Vimentin and GFAP in Cultured Human Astrocytes*

To identify the binding partner of the 14-3-3 protein in human astrocytes, we performed a protein overlay anal-

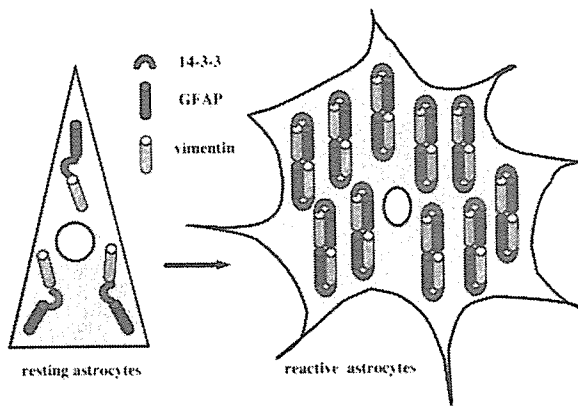


**Figure 11.** Putative role of the 14-3-3 protein in reactive gliosis in MS. Reactive gliosis is characterized by hypertrophy and proliferation of astrocytes associated with enhanced expression of GFAP (green) and vimentin (orange), which are co-polymerized in assembled filaments. Cultured human astrocytes expressed  $\beta$ ,  $\gamma$ ,  $\epsilon$ ,  $\zeta$ ,  $\eta$ , and  $\theta$  isoforms, whose levels were markedly up-regulated under the growth-promoting culture condition, in which the 14-3-3 protein (red) interacted with vimentin (orange) and GFAP (green). These observations suggest that the 14-3-3 protein (red) might act as an adaptor that connects vimentin (orange) and GFAP (green) in reactive astrocytes at the site of demyelinating lesions in MS.

ysis using recombinant human 14-3-3 $\epsilon$  protein with the Xpress tag (rh14-3-3 $\epsilon$ ) as a probe. Human astrocytes were incubated in 10% FBS-containing culture medium. Total protein extract was separated on a two-dimensional PAGE gel (Figure 8A, a) and transferred onto a polyvinylidene difluoride membrane (Figure 8A, b to h). The rh14-3-3 $\epsilon$  probe strongly reacted with several spots on the blot, among which two major 54-kD spots were designated spots no. 1 and no. 2 (Figure 8A, b). In contrast, the rhISG15 probe did not react with these spots, excluding nonspecific binding of rh14-3-3 $\epsilon$  via the Xpress tag (Figure 8A, h). Spots no. 1 and no. 2 were excised from the original gels, trypsinized, and processed for nanoESI-MS/MS analysis (Figure 9A). Among the peaks detected, eight peptide fragments derived from spot no. 1 and six from spot no. 2 showed a perfect match with the amino acid sequence covering residues 51 to 466 of human vimentin (Figure 9B), suggesting that these spots correspond to nearly full-length vimentin. Intense vimentin immunoreactivity was also identified in reactive astrocytes in demyelinating lesions of MS (Figure 3f). Furthermore, anti-vimentin monoclonal antibody reacted with spots no. 1 and no. 2, although this antibody labeled three additional, more acidic spots having smaller molecular weights (Figure 8A, c). The latter might represent post-translationally modified isoforms or degradation products of vimentin. Because vimentin is heavily phosphorylated at multiple serine residues in various mesenchymal cells, the phosphorylation state was characterized by repeated relabeling of the blot with three different antibodies specific for phosphorylated serine epitopes of vimentin. Phosphorylated Ser-39-, Ser-72-, and Ser-83-specific antibodies strongly reacted with spots no. 1 and no. 2, along with three additional spots unlabeled with rh14-3-3 $\epsilon$ , suggesting that these serine residues are not involved in the interaction of the  $\epsilon$  isoform with vimentin (Figure 8A, d to f). Protein overlay analysis using the rh14-3-3 $\epsilon$  probe

identified a distinct spot, designated spot no. 3 (Figure 8A, b). This spot was labeled with anti-GFAP antibody, indicating that GFAP is another binding partner of the 14-3-3 protein (Figure 8A, g). A more acidic spot having a smaller molecular weight immunoreactive for GFAP and weakly labeled with rh14-3-3 $\epsilon$  might represent a post-translationally modified isoform or a degradation product of GFAP (Figure 8A, b and g). Vimentin and GFAP were detected in the immunoprecipitates of cultured human astrocyte protein extract, when the lysate was incubated with the  $\epsilon$ ,  $\beta$ , or  $\zeta$  isoform-specific antibody (Figure 8B, top and bottom panels, lanes 1 to 3, 6 to 8). In contrast, only marginal bands were found in those with normal rabbit IgG (Figure 8B, top and bottom panels, lanes 4 and 9). Co-expression of the  $\epsilon$  isoform with vimentin and GFAP was verified in cultured human astrocytes (Figure 10; a to d) and in reactive astrocytes in demyelinating lesions of MS (Figure 10, e and f) by double immunolabeling.

### Discussion

The present study showed that seven 14-3-3 isoforms are differentially expressed in reactive astrocytes in demyelinating lesions of MS. Human astrocytes in culture also expressed  $\beta$ ,  $\gamma$ ,  $\epsilon$ ,  $\zeta$ ,  $\eta$ , and  $\theta$  isoforms whose levels were markedly elevated under the growth-promoting culture condition. In demyelinating lesions of MS, the majority of GFAP<sup>+</sup> hypertrophic astrocytes intensely expressed  $\beta$ ,  $\epsilon$ ,  $\zeta$ , and  $\eta$  isoforms, although the expression of these isoforms was found in reactive astrocytes appearing in non-MS brains. Previous studies showed that the  $\sigma$  isoform expression is confined to differentiated squamous epithelial cells.<sup>19,38</sup> However, we found that some reactive astrocytes in MS and non-MS brains intensely expressed this isoform. Neurons constitutively expressed  $\beta$ ,  $\gamma$ ,  $\zeta$ , and  $\eta$  isoforms but they did not constantly express  $\epsilon$  or  $\sigma$  isoforms. Macrophages and microglia in MS and non-MS lesions intensely expressed  $\beta$ ,  $\zeta$ , and  $\eta$  isoforms, but they did not express  $\epsilon$ ,  $\theta$ , or  $\sigma$  isoforms. A substantial population of oligodendrocytes, surviving in active demyelinating lesions of MS and ischemic lesions of cerebral infarction, intensely expressed the  $\theta$  isoform, consistent with the expression of this isoform in the white matter of the developing rat CNS.<sup>7</sup> These observations are in agreement with our previous findings that the 14-3-3 protein is expressed not only in neurons but also in astrocytes, microglia, and oligodendrocytes in mouse brain cell cultures.<sup>26</sup> The present observations suggest that up-regulated expression of the  $\epsilon$  isoform could be used as an immunohistochemical marker to identify reactive astrocytes at least in demyelinating lesions of MS and ischemic lesions of cerebral infarction. However, Lewy bodies in the Parkinson's disease brain<sup>30</sup> and a minor population of neurons in MS and non-MS brains express the  $\epsilon$  isoform, indicating that this isoform is not astrocyte-specific.

The biological role of  $\epsilon$  and  $\sigma$  isoforms in human astrocyte function remains unknown. Increasing evidence indicates that isoform-specific function regulates the devel-

opment and differentiation of neural and nonneural cells. Particularly, the  $\epsilon$  isoform plays a role in the regulation of various cellular signaling events. The 14-3-3 $\epsilon$  gene is deleted in the patients with Miller-Dieker syndrome, a human neuronal migration disorder presenting with the most severe form of lissencephaly (LIS) associated with facial abnormalities.<sup>39</sup>  $\epsilon$  Isoform-deficient mice are defective in neuronal migration during brain development.<sup>40</sup> The multimolecular complex composed of the  $\epsilon$  isoform, LIS1 and nudE nuclear distribution gene E homolog-like 1 (NUDEL) regulates the activity of dynein, a cytoplasmic motor protein, suggesting a role of  $\epsilon$  in neuronal migration.<sup>40</sup> Somatic homozygous deletion of the 14-3-3 $\epsilon$  gene is frequently found in small cell lung cancers, supporting the idea that the  $\epsilon$  isoform serves as a tumor suppressor gene.<sup>41</sup> The 14-3-3 $\epsilon$  isoform, by binding to the intracellular domain of the p75 neurotrophin receptor (NTR) in a NGF-dependent manner, promotes p75NTR-associated cell death executor (NADE)-mediated apoptosis.<sup>42</sup> During apoptosis, the  $\epsilon$  protein is cleaved by caspase-3 at a cleavage site located in the C-terminal hydrophobic tail, where the amino acid sequence is highly variable among different 14-3-3 isoforms.<sup>43</sup> The  $\epsilon$  isoform interacts with cdc25A and cdc25B phosphatases, key enzymes required for cell-cycle progression by activating cyclin-dependent kinases.<sup>44</sup> Phosphorylation-dependent interaction of the  $\epsilon$  isoform with heat shock transcription factor HSF1 restricts the location of HSF1 in the cytoplasm by keeping it in an inactive form.<sup>45</sup> The  $\epsilon$  isoform catalyzes the depolymerization and unfolding of mitochondrial precursor proteins in an ATP-dependent manner.<sup>46</sup> Based on these observations, we propose that the  $\epsilon$  isoform plays a regulatory role in proliferation, apoptosis, and stress responses in reactive astrocytes.

The  $\sigma$  isoform constitutes a component of the G<sub>2</sub>/M cell-cycle checkpoint machinery.<sup>47</sup> Exposure of the cells to DNA-damaging agents results in p53-dependent induction of the  $\sigma$  isoform, which in turn arrests the cells in the G<sub>2</sub>/M phase by sequestering the cdc2-cyclin B1 complex in the cytoplasm.<sup>48</sup> Therefore,  $\sigma$  isoform-deficient cells are unable to maintain cell-cycle arrest.<sup>47</sup> Selective down-regulation of the  $\sigma$  isoform because of the hypermethylation of CpG islands in its promoter region is responsible for the malignant transformation of breast cancer cells,<sup>49</sup> whereas reduced expression of the  $\sigma$  isoform allows human epidermal keratinocytes to escape replicative senescence.<sup>50</sup> These observations raise the possibility that a population of reactive astrocytes with strong immunoreactivity against the  $\sigma$  isoform might represent the cells responding to DNA damage at the site of demyelinating lesions in MS and ischemic lesions of cerebral infarction.

Reactive gliosis is characterized by hypertrophy and proliferation of astrocytes associated with enhanced expression of GFAP and vimentin, accompanied by increased production of growth factors, cytokines, neuropeptides, and extracellular matrix molecules.<sup>51,52</sup> Astrocytes play a role in the repair of the blood-brain barrier, protection of neurons from glutamate excitotoxicity, and enhancement of neuronal survival by supplying neurotrophic factors.<sup>53</sup> On the other hand, reactive astro-

cytes strongly inhibit neurite outgrowth by forming glial scars after CNS injury and inflammation.<sup>53,54</sup> Through protein overlay and nanoESI-MS/MS analysis, we showed that vimentin is the major 14-3-3 protein-interacting protein expressed in cultured human astrocytes. Consistent with previous observations,<sup>55,56</sup> we identified vimentin expression in reactive astrocytes in demyelinating lesions of MS. Astrocytes isolated from vimentin-deficient mice possess an abnormal filamentous network of GFAP.<sup>57,58</sup> Furthermore, mice lacking vimentin and GFAP do not form proper glial scars after CNS injury, indicating that the type III IF family proteins play a pivotal role in cytoskeletal organization in astrocytes.<sup>59</sup>

In our study, the rh14-3-3 $\epsilon$  probe strongly reacted with two distinct spots named no. 1 and no. 2 among five phosphovimentin-immunoreactive spots on the blot. Vimentin was immunoprecipitated with the  $\zeta$  and  $\beta$  isoforms along with  $\epsilon$ . These observations suggest that the interaction between vimentin and the 14-3-3 protein is not isoform-specific, and that the 14-3-3 protein-binding domain in vimentin might not include phosphorylated Ser-39, Ser-72, and Ser-83 epitopes. Protein overlay analysis identified GFAP as another binding partner of the 14-3-3 $\epsilon$  isoform. Immunoprecipitation experiments verified the interaction between GFAP and the  $\epsilon$ ,  $\zeta$ , or  $\beta$  isoform. However, a different spot strongly immunoreactive against GFAP but much weakly labeled with rh14-3-3 $\epsilon$  was identified on the two-dimensional gel blot. This suggests that a substantial pool of cytoplasmic vimentin and GFAP proteins steadily interact with the 14-3-3 protein in human astrocytes.

Our observations raise the possibility that the 14-3-3 protein acts as an adaptor that connects vimentin and GFAP in cultured human astrocytes (Figure 11). Previous studies showed that vimentin and GFAP are co-expressed and co-polymerized in assembled filaments in astrocytes,<sup>56,60</sup> supporting the view that the 14-3-3 protein not only bridges vimentin and GFAP one by one, but also bundles both of them in the same assembled filaments. All these proteins are expressed at much higher levels in reactive astrocytes, which require more efforts to coordinate the IF network compared with resting astrocytes (Figure 11). Several other binding partner candidates for vimentin in astrocytes include  $\alpha$ -crystallin, which inhibits the *in vitro* assembly of GFAP,<sup>61</sup> and the multiple endocrine neoplasia type 1 (MEN1) gene product named menin, which binds to vimentin and GFAP in glioma cells.<sup>62</sup> The 14-3-3 $\gamma$  isoform interacts with F-actin and Raf kinase in cultured mouse astrocytes, indicating its role in cytoskeletal rearrangement during cell growth and division.<sup>63,64</sup> Importantly, a recent study using COS-7 cells overexpressing the 14-3-3 protein showed that phosphorylated vimentin binds to the 14-3-3 protein and limits the interaction of 14-3-3 with other 14-3-3-binding partners, thereby modulating Raf-dependent intracellular signaling.<sup>65</sup> This study also found that vimentin does not have typical consensus 14-3-3-binding motifs.<sup>65</sup> However, a close interaction of the 14-3-3 protein with phosphorylated vimentin affects the phosphorylation and dephosphorylation state of vimentin.<sup>65</sup> Site-specific phosphorylation of vimentin and GFAP is mediated by



a range of protein kinases, including Rho kinase, cdc2 kinase, Ca<sup>2+</sup> calmodulin-dependent kinase II, protein kinases A and C, and Aurora-B kinase.<sup>60,66–69</sup> They coordinately regulate dynamic equilibrium between the assembly and disassembly of IF proteins during mitosis.<sup>60,66–69</sup> Furthermore, these kinases are identified as binding partners for the 14-3-3 protein.<sup>1–3</sup> Therefore, our observations suggest that the 14-3-3 protein plays a role in the organization of IF proteins and IF-related kinases during conversion from resting astrocytes to reactive astrocytes. A role for 14-3-3 protein in IF dynamics is supported by our preliminary observations that suggest the effects of difopein,<sup>70</sup> a specific inhibitor of 14-3-3 protein/ligand interaction, on the morphological characteristics of cultured human astrocytes.

### Acknowledgments

We thank Dr. Mitsuru Kawai, Department of Neurology, National Center Hospital for Mental, Nervous, and Muscular Disorders, NCNP, Tokyo, Japan, for providing information about MS patients; Dr. Toshikazu Murakami, Department of Pathology, Kohnodai Hospital, NCNP, Chiba, Japan, for providing the brains of neurologically normal controls; Drs. Kazuhiko Watabe and S.U. Kim, University of British Columbia, Vancouver, BC, Canada, for providing cultured fetal human astrocytes; and Dr. Masashi Fukuda, Invitrogen Proteome, Yokohama, Japan, for his help in nanoESI-MS/MS analysis.

### References

1. Fu H, Subramanian RR, Masters SC: 14-3-3 proteins: structure, function, and regulation. *Annu Rev Pharmacol Toxicol* 2000, 40:617–647
2. van Hemert MJ, Steensma HY, van Heusden GPH: 14-3-3 proteins: key regulators of cell division, signaling and apoptosis. *Bioessays* 2001, 23:936–947
3. Aitken A, Baxter H, Dubois T, Cloukie S, Mackie S, Mitchell K, Peden A, Zemlickova E: 14-3-3 proteins in cell regulation. *Biochem Soc Trans* 2002, 30:351–360
4. Berg D, Holzmann C, Riess O: 14-3-3 proteins in the nervous system. *Nature Rev Neurosci* 2002, 4:752–762
5. Boston PF, Jackson P, Kyonocho PAM, Thompson RJ: Purification, properties, and immunohistochemical localization of human brain 14-3-3 protein. *J Neurochem* 1982, 38:1466–1474
6. Watanabe M, Isobe T, Ichimura T, Kuwano R, Takahashi Y, Kondo H: Molecular cloning of rat cDNAs for  $\beta$  and  $\gamma$  subtypes of 14-3-3 protein and developmental changes in expression of their mRNAs in the nervous system. *Mol Brain Res* 1993, 17:135–146
7. Watanabe M, Isobe T, Ichimura T, Kuwano R, Takahashi Y, Kondo H, Inoue Y: Molecular cloning of rat cDNAs for the  $\zeta$  and  $\theta$  subtypes of 14-3-3 protein and differential distributions of their mRNAs in the brain. *Mol Brain Res* 1994, 25:113–121
8. Muslin AJ, Xing H: 14-3-3 proteins: regulation of subcellular localization by molecular interference. *Cell Signal* 2000, 12:703–709
9. Yaffe MB: How do 14-3-3 proteins work?—gatekeeper phosphorylation and the molecular anvil hypothesis. *FEBS Lett* 2002, 513:53–57
10. Tzivion C, Avruch J: 14-3-3 proteins: active cofactors in cellular regulation by serine/threonine phosphorylation. *J Biol Chem* 2002, 277:3061–3064
11. Zhai J, Lin H, Shamim M, Schlaepfer WW, Cañete-Soler R: Identification of a novel interaction of 14-3-3 with p190RhoGEF. *J Biol Chem* 2001, 276:41318–41324
12. Dai J-G, Murakami K: Constitutively and autonomously active protein kinase C associated with 14-3-3  $\zeta$  in the rodent brain. *J Neurochem* 2003, 84:23–34
13. Broadie K, Rushton E, Skoulakis EMC, Davis RL: Leonardo, a Drosophila 14-3-3 protein involved in learning, regulates presynaptic function. *Neuron* 1997, 19:391–402
14. Meller N, Liu Y-C, Collins TL, Bonnefoy-Bérard N, Naier G, Isakov N, Altman A: Direct interaction between protein kinase C $\theta$  (PKC $\theta$ ) and 14-3-3 $\tau$  in T cells: 14-3-3 overexpression results in inhibition of PKC $\theta$  translocation and function. *Mol Cell Biol* 1996, 16:5782–5791
15. Craparo A, Freund R, Gustafson TA: 14-3-3 ( $\epsilon$ ) interacts with the insulin-like growth factor I receptor and insulin receptor substrate 1 in a phosphoserine-dependent manner. *J Biol Chem* 1997, 272:11663–11669
16. Vincenz C, Dixit VM: 14-3-3 proteins associate with A20 in an isoform-specific manner and function both as chaperone and adaptor molecules. *J Biol Chem* 1996, 271:20029–20034
17. Wakui H, Wright APH, Gustafsson J-A, Zilliacus J: Interaction of the ligand-activated glucocorticoid receptor with the 14-3-3 $\eta$  protein. *J Biol Chem* 1997, 272:8153–8156
18. Hashiguchi M, Sobue K, Paudel HK: 14-3-3 $\zeta$  is an effector of tau protein phosphorylation. *J Biol Chem* 2000, 275:25247–25254
19. Leffers H, Madsen P, Rasmussen HH, Honoré B, Andersen AH, Walbum E, Vandekerckhove J, Celis JE: Molecular cloning and expression of the transformation sensitive epithelial marker stratifin. A member of a protein family that has been involved in the protein kinase C signaling pathway. *J Mol Biol* 1993, 231:982–998
20. Martin H, Rostas J, Patel Y, Aitken A: Subcellular localisation of 14-3-3 isoforms in rat brain using specific antibodies. *J Neurochem* 1994, 63:2259–2265
21. Baxter HC, Liu W-G, Forster JL, Aitken A, Fraser JR: Immunolocalisation of 14-3-3 isoforms in normal and scrapie-infected murine brain. *Neuroscience* 2002, 109:5–14
22. Hsieh G, Kenney K, Gibbs Jr CJ, Lee KH, Harrington MG: The 14-3-3 brain protein in cerebrospinal fluid as a marker for transmissible spongiform encephalopathies. *N Engl J Med* 1996, 335:924–930
23. Zerr I, Bodemer M, Gefeller O, Otto M, Poser S, Wiltfang J, Windl O, Kretzschmar HA, Weber T: Detection of 14-3-3 protein in the cerebrospinal fluid supports the diagnosis of Creutzfeldt-Jakob disease. *Ann Neurol* 1998, 43:32–40
24. Wiltfang J, Otto M, Baxter HC, Bodemer M, Steinacker P, Bahn E, Zerr I, Kornhuber J, Kretzschmar HA, Poser S, Rütger E, Aitken A: Isoform pattern of 14-3-3 proteins in the cerebrospinal fluid of patients with Creutzfeldt-Jakob disease. *J Neurochem* 1999, 73:2485–2490
25. Richard M, Biacabe A-G, Streichenberger N, Ironside JW, Mohr M, Kopp N, Perret-Liaudet A: Immunohistochemical localization of 14-3-3  $\zeta$  protein in amyloid plaques in human spongiform encephalopathies. *Acta Neuropathol* 2003, 105:296–302
26. Satoh J, Kurohara K, Yukitake M, Kuroda Y: The 14-3-3 protein detectable in the cerebrospinal fluid of patients with prion-unrelated neurological diseases is expressed constitutively in neurons and glial cells in culture. *Eur Neurol* 1999, 41:216–225
27. Satoh J, Yukitake M, Kurohara K, Takashima H, Kuroda Y: Detection of the 14-3-3 protein in the cerebrospinal fluid of Japanese multiple sclerosis patients presenting with severe myelitis. *J Neurol Sci* 2003, 212:11–20
28. Layfield R, Fergusson J, Aitken A, Lowe J, Landon M, Mayer RJ: Neurofibrillary tangles of Alzheimer's disease brains contain 14-3-3 proteins. *Neurosci Lett* 1996, 209:57–60
29. Agarwal-Mawal A, Qureshi HY, Cafferty PW, Yuan Z, Han D, Lin R, Paudel HK: 14-3-3 connects glycogen synthase kinase-3 $\beta$  to tau within a brain microtubule-associated tau phosphorylation complex. *J Biol Chem* 2003, 278:12722–12728
30. Berg D, Riess O, Bornemann A: Specification of 14-3-3 proteins in Lewy bodies. *Ann Neurol* 2003, 54:135
31. Ostrovskaya N, Petrucelli L, Farrer M, Mehta N, Choi P, Hardy J, Wolozin B:  $\alpha$ -Synuclein shares physical and functional homology with 14-3-3 proteins. *J Neurosci* 1999, 19:5782–5791
32. Xu J, Kao S-Y, Lee FJS, Song W, Jin L-W, Yanker BA: Dopamine-dependent neurotoxicity of  $\alpha$ -synuclein: a mechanism for selective neurodegeneration in Parkinson disease. *Nat Med* 2002, 8:600–606
33. Chen H-K, Fernandez-Funez P, Acevedo SF, Lam YC, Kaytor MD, Fernandez MH, Aitken A, Skoulakis EMC, Orr HT, Bojas J, Zoghbi HY: Interaction of Akt-phosphorylated ataxin-1 with 14-3-3 mediates neurodegeneration in spinocerebellar ataxia type 1. *Cell* 2003, 113:457–468

34. Malaspina A, Kaushik N, de Bellerocche J: A 14-3-3 mRNA is up-regulated in amyotrophic lateral sclerosis spinal cord. *J Neurochem* 2000, 75:2511-2520
35. Carpenter MK, Cui X, Hu Z-Y, Jackson J, Sherman S, Seiger A, Wahlberg LU: In vitro expansion of a multipotent population of human neural progenitor cells. *Exp Neurol* 1999, 158:262-276
36. Satoh J, Kuroda Y: Differential gene expression between human neurons and neuronal progenitor cells in culture: an analysis of arrayed cDNA clones in Ntera2 human embryonal carcinoma cell line as a model system. *J Neurosci Methods* 2000, 94:155-164
37. Loeb KR Haas AL: Conjugates of ubiquitin cross-reactive protein distribute in a cytoskeletal pattern. *Mol Cell Biol* 1994, 14:8408-8419
38. Prasad GL, Valverius EM, McDuffie E, Cooper HL: Complementary DNA cloning of a novel epithelial cell marker protein, HME1, that may be down-regulated in neoplastic mammary cells. *Cell Growth Differ* 1992, 3:507-513
39. Cardoso C, Leventer RJ, Ward HL, Toyo-oka K, Chung J, Gross A, Martin CL, Allanson J, Pitz DT, Olney AH, Murchinick OM, Hirotsune S, Wynshaw-Boris A, Dobyns WB, Ledbetter DH: Refinement of a 400-kb critical region allows genotypic differentiation between isolated lissencephaly, Miller-Dieker syndrome, and other phenotypes secondary to deletions of 17p13.3. *Am J Hum Genet* 2003, 72:918-930
40. Toyo-Oka K, Shinoya A, Gambello MJ, Cardoso C, Levenier R, Ward HL, Ayala R, Tsai L-H, Dobyns W, Ledbetter D, Hirotsune S, Wynshaw-Boris A: 14-3-3 $\epsilon$  is important for neuronal migration by binding to NUDEL: a molecular explanation for Miller-Dieker syndrome. *Nat Genet* 2003, 34:274-285
41. Konishi H, Nakagawa T, Harano T, Mizuno K, Saito H, Masuda A, Matsuda H, Osada H, Takahashi T: Identification of frequent G<sub>2</sub> checkpoint impairment and a homozygous deletion of 14-3-3 $\epsilon$  at 17p13.3 in small cell lung cancers. *Cancer Res* 2002, 62:271-276
42. Kimura MT, Irie S, Shoji-Hoshino S, Mukai J, Nadeo D, Oshimura M, Sato T-A: 14-3-3 is involved in p75 neurotrophin receptor-mediated signal transduction. *J Biol Chem* 2001, 276:17291-17300
43. Won J, Kim DY, La M, Kim D, Meadows GG, Joe CO: Cleavage of 14-3-3 protein by caspase-3 facilitates Bad interaction with Bcl-x(L) during apoptosis. *J Biol Chem* 2003, 278:19347-19351
44. Conklin DS, Galaktionov K, Beach D: 14-3-3 proteins associate with cdc25 phosphatases. *Proc Natl Acad Sci USA* 1995, 92:7892-7896
45. Wang X, Grammatikakis N, Siganou A, Calderwood SK: Regulation of molecular chaperone gene transcription involves the serine phosphorylation, 14-3-3 $\epsilon$  binding, and cytoplasmic sequestration of heat shock factor 1. *Mol Cell Biol* 2003, 23:6013-6026
46. Alam R, Hachiya N, Sakaguchi M, Kawabata S-I, Iwanaga S, Kitajima M, Mihara K, Omura T: cDNA cloning and characterization of mitochondrial import stimulation factor (MSF) purified from rat liver cytosol. *J Biochem* 1994, 116:416-425
47. Chan TA, Hermeking H, Lengauer C, Kinzler KW, Vogelstein B: 14-3-3 $\sigma$  is required to prevent mitotic catastrophe after DNA damage. *Nature* 1999, 401:616-620
48. Hermeking H, Lengauer C, Polyak K, He T-C, Zhang L, Thiagalingam S, Kinzler KW, Vogelstein B: 14-3-3 $\sigma$  is a p53-regulated inhibitor of G2/M progression. *Mol Cell* 1997, 1:3-11
49. Ferguson AT, Evaron E, Umbricht CB, Pandita TK, Chan TA, Hermeking H, Marks JR, Lambers AR, Futreal PA, Stampfer MR, Sukumar S: High frequency of hypermethylation at the 14-3-3 $\sigma$  locus leads to gene silencing in breast cancer. *Proc Natl Acad Sci USA* 2000, 97:6049-6054
50. Dellambra E, Golisano O, Bondanza S, Siviero E, Lacal P, Molinari M, D'Atri S, De Luca M: Downregulation of 14-3-3 $\sigma$  prevents clonal evolution and leads to immortalization of primary human keratinocytes. *J Cell Biol* 2000, 149:1117-1129
51. Mucke L, Eddleston M: Astrocytes in infectious and immune-mediated diseases of the central nervous system. *EMBO J* 1993, 7:1226-1232
52. Rider JL, Malhotra SK, Privat A, Gage FH: Reactive astrocytes: cellular and molecular cues to biological function. *Trends Neurosci* 1997, 20:570-577
53. Bush TG, Puvanachandra N, Horner CH, Polito A, Ostensfeld T, Svendsen CN, Mucke L, Johnson MH, Sofroniew MV: Leukocyte infiltration, neuronal degeneration, and neurite outgrowth after ablation of scar-forming, reactive astrocytes in adult transgenic mice. *Neuron* 1999, 23:297-308
54. Menet V, Ribotta MGY, Chauvet N, Drien MJ, Lanfroy J, Colucci-Guyon E, Privat A: Inactivation of the glial fibrillary acidic protein gene, but not that of vimentin, improves neuronal survival and neurite growth by modifying adhesion molecule expression. *J Neurosci* 2001, 21:6147-6158
55. Yamada T, Kawamata T, Walker DG, McGeer PL: Vimentin immunoreactivity in normal and pathological human brain tissues. *Acta Neuropathol* 1992, 84:157-162
56. Holley JE, Gveric D, Newcombe J, Cuzner ML, Gutowski NJ: Astrocyte characterization in the multiple sclerosis glial scar. *Neuropathol Appl Neurobiol* 2003, 29:434-444
57. Galou M, Solucci-Guyon E, Ensergueix D, Rider J-L, Robotta MGY, Privat A, Babinet C, Dupouey P: Disrupted glial fibrillary acidic protein network in astrocytes from vimentin knockout mice. *J Cell Biol* 1996, 133:853-863
58. Eliasson C, Sahlgrens C, Berthold C-H, Stakeberg J, Celis JE, Betsholtz C, Eriksson JE, Pekny M: Intermediate filament protein partnership in astrocytes. *J Biol Chem* 1999, 274:23996-24006
59. Pekny M, Johansson B, Eliasson C, Stakeberg J, Wallén A, Perlmann T, Lendahl U, Betsholtz C, Berthold C-H, Frisén J: Abnormal reaction to central nervous system injury in mice lacking glial fibrillary acidic protein and vimentin. *J Cell Biol* 1999, 145:503-514
60. Inagaki M, Nakamura Y, Takeda M, Nishimura T, Inagaki N: Glial fibrillary acidic protein: dynamic property and regulation by phosphorylation. *Brain Pathol* 1994, 4:239-243
61. Nicholl ID, Quinlan RA: Chaperone activity of  $\alpha$ -crystallins modulates intermediate filament assembly. *EMBO J* 1994, 13:945-953
62. Lopez-Egido JR, Cunningham J, Berg M, Oberg K, Bongcam-Rudloff E, Gobl AE: Menin's interaction with glial fibrillary acidic protein and vimentin suggests a role for the intermediate filament network in regulating menin activity. *Exp Cell Biol* 2002, 278:175-183
63. Chen XQ, Yu ACH: The association of 14-3-3 $\gamma$  and actin plays a role in cell division and apoptosis in astrocytes. *Biochem Biophys Res Commun* 2002, 296:657-663
64. Chen XQ, Chen JG, Zhang Y, Hsiao WWL, Yu ACH: 14-3-3 $\gamma$  is upregulated by in vitro ischemia and binds to protein kinase Raf in primary cultures of astrocytes. *Glia* 2003, 42:315-324
65. Tzivion G, Luo Z-J, Avruch J: Calyculin A-induced vimentin phosphorylation sequesters 14-3-3 and displaces other 14-3-3 partners in vivo. *J Biol Chem* 2000, 275:29772-29776
66. Tsujimura K, Tanaka J, Ando S, Matsucka Y, Kusubata M, Sugiura H, Yamauchi T, Inagaki M: Identification of phosphorylation sites on glial fibrillary acidic protein for cdc2 kinase and Ca<sup>2+</sup>-calmodulin-dependent protein kinase II. *J Biochem* 1994, 116:426-434
67. Goto H, Kosako H, Tanabe K, Yanagida M, Sakurai M, Amano M, Kaibuchi K, Inagaki M: Phosphorylation of vimentin by Rho-associated kinase at a unique amino-terminal site that is specifically phosphorylated during cytokinesis. *J Biol Chem* 1996, 273:11726-11738
68. Takemura M, Gomi H, Colucci-Guyon E, Itohara S: Protective role of phosphorylation in turnover of glial fibrillary acidic protein in mice. *J Neurosci* 2002, 22:6972-6979
69. Goto H, Yasui Y, Kawajiri A, Nigg EA, Terada Y, Tatsuka M, Nagata K-I, Inagaki M: Aurora-B phosphorylates the cleavage furrow-specific vimentin phosphorylation in the cytokinetic process. *J Biol Chem* 2003, 278:8526-8530
70. Masters SC, Fu H: 14-3-3 proteins mediate an essential anti-apoptotic signal. *J Biol Chem* 2001, 276:45193-45200

# More sympathy for autoimmunity with neuropeptide Y?

Sammy Bedoui<sup>1</sup>, Sachiko Miyake<sup>3</sup>, Rainer H. Straub<sup>2</sup>, Stephan von Hörsten<sup>1</sup> and Takashi Yamamura<sup>3</sup>

<sup>1</sup>Department of Functional and Applied Anatomy, Medical School of Hannover, 30625 Hannover, Germany

<sup>2</sup>Department of Internal Medicine I, University Hospital Regensburg, 93042 Regensburg, Germany

<sup>3</sup>Department of Immunology, National Institute of Neuroscience, 4-1-1 Ogawahigashi, Kodaira, Tokyo 187-8502, Japan

**Substantial evidence indicates a dysfunctional communication between the sympathetic nervous system and the immune system in Th1-mediated autoimmune diseases, such as rheumatoid arthritis and multiple sclerosis. In this Opinion, we propose that the sympathetic regulation of immunity is not only mediated by catecholamines but also involves neuropeptide Y (NPY), an additional postganglionic SNS transmitter that is shown to modulate various immunological functions *in vitro* and *in vivo*. Based on recent experimental findings, we believe that a more precise understanding of the role of NPY in the regulation of autoimmune Th1 cells will provide novel insights into the neuroimmunological basis of autoimmunity.**

The precise pathophysiological mechanisms underlying organ-specific autoimmune disorders, such as multiple sclerosis (MS) and rheumatoid arthritis (RA), are largely unknown. Therefore, it is not surprising that treatment options for these diseases still remain unsatisfactory. Despite significant variations in the pathophysiology of autoimmune diseases, it is generally accepted that CD4<sup>+</sup> Th1 lymphocytes have a key role in mediating target tissue destruction [1]. By producing typical Th1 cytokines, such as interferon- $\gamma$  (IFN- $\gamma$ ), autoimmune T lymphocytes maintain and drive complex immune responses ultimately resulting in the destruction of the body's own structures, such as myelin sheaths in the case of MS or cartilage tissues in patients with RA.

It is now well established that the sympathetic nervous system (SNS) and the immune system communicate functionally with each other [2–5]. Interestingly, recent studies have indicated that the SNS is mechanically and/or functionally affected in RA and MS [6,7], suggesting that the crosstalk between the SNS and the immune system is substantially disturbed in Th1-mediated autoimmune diseases. So far, experimental and clinical studies seeking to correlate the sympathetic defect and associated autoimmune disorders have predominantly focused on catecholamines, as they are widely considered to be the major sympathetic transmitters [8]. In fact, there is substantial evidence to suggest that catecholamines are able to suppress typical Th1-mediated autoimmune

responses [9]. This has led to the idea that catecholamines or catecholaminergic agents can be therapeutic options for the treatment of autoimmune disease. However, considerable evidence suggests that the 'adrenergic intervention' might be of limited value in providing protection against autoimmune diseases. Autoreactive T cells from patients with RA, for example, elicit significantly reduced functional responses to catecholamines due to altered expression of  $\beta$ -adrenergic receptors [10]. A further limitation is seen in the demonstration that, even though catecholamine levels in joint cavities of RA are elevated, active inflammation does not appear to be controlled [11].

Notably, catecholamines are not the only sympathetic transmitters that are of relevance for the communication between the SNS and the immune system. Postganglionic sympathetic nerves innervating primary and secondary lymphoid organs also release neuropeptide Y (NPY). Resembling the ability of other neuropeptides, such as vasointestinal peptide [12], to modulate crucial immunological functions in health and disease, NPY also has a crucial role in the communication between the SNS and the immune system [13]. In this Opinion, we will discuss the role of NPY in the regulation of autoimmunity and suggest that NPY, in addition to NPY receptor agonists and antagonists, represents an interesting innovative tool to shed new light on the pathology of Th1-mediated autoimmune diseases.

## Disturbances in the interactions between the SNS and the immune system in autoimmune disease

Early indications for a role of the SNS in modulating autoimmune responses came from studies showing that the chemical depletion of sympathetic transmitters modulates prototypical models of Th1-mediated autoimmunity, such as experimental autoimmune encephalomyelitis (EAE). Back in 1988, Chelmicka-Schorr *et al.* demonstrated that chemical sympathectomy augments disease severity of EAE induced by both active sensitization with myelin components and passive transfer of encephalitogenic T lymphocytes [14,15]. Similar results were obtained in experimental models of RA, in which chemical sympathectomy exacerbated the inflammation and osteopathic destruction of arthritic joints [16]. Although these direct observations support an anti-inflammatory role for the SNS, there are data available demonstrating that the

Corresponding author: Takashi Yamamura (yamamura@cncp.go.jp).  
Available online 20 August 2004

SNS can also be proinflammatory. This is of particular importance in experimental arthritis, where it was demonstrated that the SNS can indirectly promote the process of neurogenic inflammation by which joint damage is augmented [17].

Thus, the SNS modulates autoimmune responses in a bimodal manner: on the one hand there is a strong anti-inflammatory branch, whereas on the other hand the SNS also exerts proinflammatory action. It remains to be determined which factors are involved in the decision as to whether the pro- or the anti-inflammatory branch of the SNS predominates. One such factor could be the stage of the disease because converse effects of chemical sympathectomy have been observed in collagen-induced arthritis that was treated at different stages of the disease.

Functional defects of the SNS are not only present under experimental conditions. Clinical studies have also revealed considerable SNS dysfunction in patients with MS, such as impaired sympathetic skin responses and abnormal cardiovascular reflexes [7,18], suggesting that the defective crosstalk between the SNS and the immune system might further precipitate the manifestations of MS. In the same line of evidence, a selective reduction in sympathetic fibers has been demonstrated in the synovium of patients with RA [11]. Although it is unclear precisely how the SNS is affected in inflamed joints, the detectable changes in the SNS have been interpreted as evidence for the disruption of the local neuroimmunological control of inflammation in RA [19].

#### **Catecholamines in autoimmunity: not the whole truth?**

Based on the fact that immune cells express functional  $\beta_2$ -adrenergic receptors [2–4], several investigators have studied the significance of the  $\beta$ -adrenergic pathway in autoimmune processes. *In vivo* experiments have shown that repetitive injections of  $\beta_2$ -adrenergic agonists effectively suppress clinical manifestations of both EAE and experimental arthritis [9,15]. Furthermore, it has been reported that pharmacological stimulation of the  $\beta_2$ -adrenergic pathway promotes the induction of oral tolerance by selectively inhibiting proinflammatory cytokines, such as IFN- $\gamma$  and interleukin-12 (IL-12), as well as promoting anti-inflammatory cytokines, such as IL-4, transforming growth factor- $\beta$  and IL-1R antagonist [20].

Even though these findings raise hopes of using catecholamines and adrenergic stimulants as new therapeutic approaches, there are also concerns about introducing 'adrenergic intervention' into the clinical arena. In fact, Miller *et al.* [11] showed that despite the reduction in sympathetic fibers in the joints of RA patients, the levels of norepinephrine are remarkably normal as a result of upregulated secretion of norepinephrine from synovial TH<sup>+</sup> cells, suggesting an endogenous mechanism compensating for the loss of sympathetic innervation. Although the meaning of this observation remains speculative, it does not support the optimistic idea that further elevation of catecholamine levels leads to the suppression of inflammation.

An additional problem for an 'adrenergic intervention' comes from the well-known phenomenon of up- and downregulation of adrenergic receptors when the local

levels of catecholamines are changed [4,21]. Accordingly, altered numbers and affinities of  $\beta_2$ -adrenergic receptors have been reported for T lymphocytes from RA [22] and MS patients [23], thus changing their responsiveness to the suppressive action of catecholamines.

#### **The complexity of the humoral crosstalk between the SNS and the immune system**

A more precise look at sympathetic neurotransmission reveals that catecholamines are not the only transmitters released upon stimulation or depleted upon chemical sympathectomy. Instead, the release of catecholamines is usually accompanied by the secretion of other sympathetic mediators, such as NPY or ATP. Sympathetic transmission in general is a rather complex process, involving differential corelease sequences, direct interactions between the transmitters in the synaptic cleft and alterations in presynaptic and postsynaptic receptor sensitivity [8,24]. This complexity also accounts for the immunological actions of the SNS. Both catecholamines and NPY, for example, evoke various immunological functions independently, yet they also interact functionally. More specifically, NPY differentially regulates the functional efficacy of catecholaminergic effects during leukocyte mobilization. Weak catecholaminergic stimuli are facilitated in the presence of NPY, whereas exaggerated catecholamine effects can be inhibited [25]. Furthermore, the influence of NPY on catecholaminergic effects in the immune system also differs depending on which adrenergic receptor subtype is engaged to activate the downstream pathway [26]. Thus, NPY must be included in the picture, to improve our understanding of the precise mechanisms underlying the defective interaction between the SNS and the immune system in autoimmunity.

#### **A role for NPY in suppressing Th1-mediated autoimmunity**

NPY, a 36 amino acid peptide, was discovered in 1982 by Tatemoto and has since been found to be present in various brain regions, where it is implicated in various central nervous system functions. In the periphery, NPY is released from sympathetic nerves alone and in combination with catecholamines [24]. Interestingly, NPY has been implicated in a multitude of immunological functions and mechanisms [13]. For example, NPY increases the phagocytosis of *Candida albicans* [27], differentially regulates IL-1 $\beta$  and IL-6 secretion by monocytes [28] and modulates T-lymphocyte adhesion [29]. Of particular interest are two independent reports showing that NPY inhibits the secretion of IFN- $\gamma$  and enhances IL-4 secretion of murine lymphocytes *in vitro*, indicating that NPY shifts the Th1/Th2 balance towards the Th2 phenotype [30,31]. Together with the finding that NPY levels are decreased in the cerebrospinal fluid of MS patients [32], a role for NPY in Th1-mediated central nervous system autoimmunity seemed likely. Therefore, we tested to see whether repetitive administrations of NPY exerted any impact on EAE, and found that it ameliorated symptoms and disease severity in a dose-dependent fashion [33]. This study provided the first direct indication that a sympathetic transmitter other

than a catecholamine contributes to the 'immunoregulatory-immunoregulatory' role of the SNS in Th1-mediated autoimmunity.

Furthermore, there have been several other observations suggesting a regulatory role for NPY in human Th1-mediated autoimmunity. The potential relevance of NPY for MS was very recently emphasized in a genetic study revealing a vulnerability locus on human chromosome 7p15 [34], a locus that actually encodes NPY. Additionally, a specific loss of NPY-containing fibers was found in the synovium of RA patients [6,11], and NPY concentrations in the joints of RA patients were found to be directly correlated with symptom severity, with higher levels of NPY associated with a shorter duration of pain [35]. These observations suggest that decreased local concentrations of NPY are involved in the progression of joint inflammation in RA. It remains to be investigated whether NPY also has the ability to modulate animal models of arthritis.

#### Mechanisms by which NPY might influence Th1-mediated autoimmunity

Looking for underlying mechanisms for the suppressive action of NPY on EAE (Figure 1), we discovered that treatment with NPY changes the cytokine profile of autoreactive T lymphocytes towards the Th2 phenotype *ex vivo*. When stimulated with the specific autoantigen, autoreactive T lymphocytes from EAE mice that had been treated with NPY secreted significantly lower amounts of IFN- $\gamma$ . Another *in vivo* indicator for a deviation towards the Th2 phenotype in treated mice is the finding that the majority of autoantigen-specific antibodies are of the IgG1 isotype [33]. It was also interesting to establish whether NPY exerted its effects directly on T lymphocytes or whether it acted via an indirect action mediated by antigen-presenting cells. Using differential cocubation protocols, we were able to show that NPY acts directly on T lymphocytes via the NPY Y<sub>1</sub> receptor subtype. Thus, it is our opinion that NPY induces a shift in autoreactive T lymphocytes towards the Th2 phenotype. As the induction of a Th2 shift is also known to be beneficial in arthritis, we speculate that a possible suppressive effect of NPY on experimental or clinical arthritis could also engage this mechanism. However, such investigations must also consider other cellular targets for NPY, such as natural killer cells, macrophages, mast cells or osteoclasts, because these cells also have an important role in the pathogenesis of arthritis.

As NPY is usually secreted in combination with catecholamines, it is most likely that the cooperativity between both SNS transmitters also has a significant role in influencing autoimmune responses. NPY is known to differentially modulate the immunological effects of catecholamines. This complex phenomenon depends on such parameters as the adrenergic receptor subtype predominantly activated ( $\alpha$ - versus  $\beta$ -adrenoreceptors), and the concentrations of catecholamines actually involved. Of particular interest is the finding that low, ineffective concentrations of catecholamines can be facilitated upon coadministration of NPY. For example, when applied in combination with NPY, catecholamine dosages

that are *per se* without an effect can evoke a biological response attributable to the action of catecholamines [25]. As autoimmunity represents a situation in which the catecholaminergic action is somehow ineffective, administration of exogenous NPY might represent a mechanism for facilitating and potentiating the subthreshold action of endogenous catecholamines.

#### Ineffective activation of Y<sub>1</sub> receptors in autoimmunity?

It has been demonstrated that T lymphocytes from individuals with MS express higher amounts of the surface protein CD26 [36]. Notably, this protein is not only an activation marker but also exerts enzymatic activities, which are of major consequence for NPY [24]. The result of N-terminal truncation of NPY by CD26 is a peptide fragment with significantly altered receptor affinities, as the degradation product NPY<sub>3-36</sub> loses its ability to activate the Y<sub>1</sub> receptor and becomes a selective agonist at the Y<sub>2</sub> and Y<sub>5</sub> receptors [37]. Increased degradation of NPY by CD26 under autoimmune conditions might thus account for insufficient activation of Y<sub>1</sub> receptors, which in turn favors the development of Th1 responses. Interestingly, this possibility is consistent with the recent report that the pharmacological inhibition of CD26 suppresses the clinical course of EAE via the induction of a Th2 shift [38]. It remains to be investigated whether the suppressive action of CD26 inhibition results from increased Y<sub>1</sub> receptor activation and the corresponding Th2 shift.

Apart from the possibility of increased functional degradation of NPY and the resulting consequences for the Th1/Th2 balance of autoimmune responses, an additional mechanism might be at work to decrease the efficiency of Y<sub>1</sub> receptor activation in autoimmunity. Silva *et al.* [39] have recently reported that IFN- $\gamma$  preferentially upregulates the expression of Y<sub>5</sub> receptors without exerting any effect on the expression of Y<sub>1</sub> receptors in human umbilical cord endothelial cells. It might well be the case that the increased levels of IFN- $\gamma$  present in Th1-mediated autoimmune responses also selectively increase the expression of Y<sub>5</sub> receptors, which in turn shifts the balance between Y<sub>1</sub> and Y<sub>5</sub> receptor activation.

These indirect indications give us clues for further investigations into the role of NPY in the regulation of autoimmune processes and help us to develop pharmacological interventions for autoimmune diseases based on stimulating NPY receptors or inhibiting the degradation of NPY.

#### Conclusion and future perspective

There is convincing experimental and clinical evidence demonstrating a dysfunctional communication between the SNS and the immune system in autoimmunity. Despite the early notion that catecholamines are the main players in the sympathetic control of Th1 immunity, we show here that other sympathetic transmitters, such as NPY, also have a significant role in autoimmunity. It is our view that the catecholaminergic defect only partially reflects the pathophysiological basis of the defective crosstalk between the SNS and the immune system. A

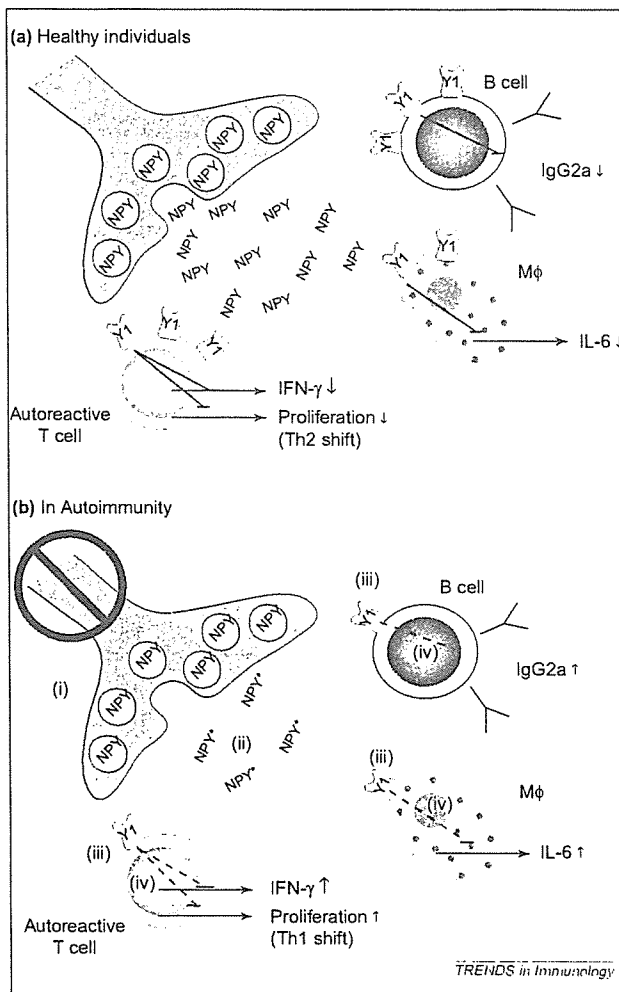


**Figure 1.** The effects of neuropeptide Y (NPY) on certain immune parameters in both physiological and autoimmune conditions. (a) Under physiological conditions, NPY is released from sympathetic nerve fibers innervating immune competent organs, such as lymph nodes and the spleen. Upon its release, NPY binds to Y<sub>1</sub> receptors, which are expressed on a variety of immune cells, where it induces functional effects, such as the promotion of Th2 responses, by inhibiting the release of interferon (IFN)- $\gamma$  from T cells and promoting the production of IgG1 antibodies. NPY also inhibits the production of proinflammatory cytokines from macrophages. (b) Proposed model of the involvement of NPY in autoimmunity. There is a loss of NPY-containing sympathetic nerve fibers (i) innervating disease-relevant compartments, such as the joint cavity in rheumatoid arthritis (RA), and a significant decrease in NPY levels (ii) in the cerebrospinal fluid from patients with multiple sclerosis (MS). In analogy to the alterations in  $\beta_2$ -adrenoreceptor expression in RA and MS, we hypothesize that the number of NPY Y<sub>1</sub> receptors (iii) and their responsiveness (iv) might also be altered. This proposed multitude of mechanisms for reducing responsiveness to NPY induces a Th1 shift, as demonstrated by increased production of IFN- $\gamma$  and IgG2a antibodies. We also speculate that in the absence of NPY, the production of interleukin-6 (IL-6) from macrophages (M $\phi$ ) is increased.

comprehensive understanding of SNS and immune system interactions during autoimmunity can only be achieved by shifting the focus towards alternative sympathetic transmitters, such as NPY or ATP, and their role in autoimmune processes.

Many issues of the complex network between the SNS and the immune system and their significance for autoimmunity remain to be clarified. What are the precise mechanisms and factors that determine whether the anti-inflammatory or the proinflammatory branch of the SNS predominates? What is the role of other SNS transmitters,

such as ATP? How do non-immunological properties, such as the angiogenic properties of the SNS [40], contribute to this network?

Solving these issues might prove to be a stimulus for reigniting the possibility of a 'sympathetic intervention' for autoimmune disorders.

#### Acknowledgements

We are grateful for the inspiration and critical comments of Reinhard Pabst. We also gratefully acknowledge the contribution of S. Fryk for correcting our English.

#### References

- Liblau, R.S. *et al.* (1995) Th1 and Th2 CD4<sup>+</sup> T cells in the pathogenesis of organ-specific autoimmune diseases. *Immunol. Today* 16, 34–38
- Straub, R.H. *et al.* (1998) Dialogue between the CNS and the immune system in lymphoid organs. *Immunol. Today* 19, 409–413
- Kohm, A.P. and Sanders, V.M. (2001) Norepinephrine and  $\beta_2$ -adrenergic receptor stimulation regulate CD4<sup>+</sup> T and B lymphocyte function *in vitro* and *in vivo*. *Pharmacol. Rev.* 53, 487–525
- Elenkov, L.J. *et al.* (2000) The sympathetic nerve – an integrative interface between two supersystems: the brain and the immune system. *Pharmacol. Rev.* 52, 595–638
- Bedoui, S. *et al.* (2003) Relevance of neuropeptide Y for the neuroimmune crosstalk. *J. Neuroimmunol.* 134, 1–11
- Mapp, P.I. *et al.* (1990) Substance P-, calcitonin gene-related peptide- and C-flanking peptide of neuropeptide Y-immunoreactive fibres are present in normal synovium but depleted in patients with rheumatoid arthritis. *Neuroscience* 37, 143–153
- Nordenbo, A.M. *et al.* (1989) Cardiovascular autonomic function in multiple sclerosis. *J. Auton. Nerv. Syst.* 26, 77–84
- Lundberg, J.M. (1996) Pharmacology of cotransmission in the autonomic nervous system: integrative aspects on amines, neuropeptides, adenosine triphosphate, amino acids and nitric oxide. *Pharmacol. Rev.* 48, 113–178
- Malfait, A.M. *et al.* (1999) The  $\beta_2$ -adrenergic agonist salbutamol is a potent suppressor of established collagen-induced arthritis: mechanisms of action. *J. Immunol.* 162, 6278–6283
- Baerwald, C.G. *et al.* (1997) Impaired sympathetic influence on the immune response in patients with rheumatoid arthritis due to lymphocyte subset-specific modulation of  $\beta_2$ -adrenergic receptors. *Br. J. Rheumatol.* 36, 1262–1269
- Miller, L.E. *et al.* (2000) The loss of sympathetic nerve fibers in the synovial tissue of patients with rheumatoid arthritis is accompanied by increased norepinephrine release from synovial macrophages. *FASEB J.* 14, 2097–2107
- Delgado, M. (2003) VIP: a very important peptide in T helper differentiation. *Trends Immunol.* 24, 221–224
- Bedoui, S. *et al.* (2004) NPY and immune functions: implications for health and disease. In *Handbook of Pharmacology* (Vol. 162) (Michel, M., ed.), pp. 404–445, Springer Press
- Chelmicka-Schorr, E. *et al.* (1988) Chemical sympathectomy augments the severity of experimental allergic encephalomyelitis. *J. Neuroimmunol.* 17, 347–350
- Wiegmann, K. *et al.* (1995)  $\beta$ -adrenergic agonists suppress chronic/relapsing experimental allergic encephalomyelitis (CREAE) in Lewis rats. *J. Neuroimmunol.* 56, 201–206
- Lorton, D. *et al.* (1996) Application of 6-hydroxydopamine into the fatpads surrounding the draining lymph nodes exacerbates adjuvant-induced arthritis. *J. Neuroimmunol.* 64, 103–113
- Levine, J.D. *et al.* (1987) Contribution of the nervous system to the pathophysiology of rheumatoid arthritis and other polyarthritides. *Rheum. Dis. Clin. North Am.* 13, 369–383
- Lachenecker, P. *et al.* (2001) Autonomic dysfunction in multiple sclerosis is related to disease activity and progression of disability. *Mult. Scler.* 7, 327–334
- Levine, J.D. *et al.* (1985) Hypothesis: the nervous system may contribute to the pathophysiology of rheumatoid arthritis. *J. Rheumatol.* 12, 406–411

- 20 Cobelens, P.M. *et al.* (2002) The  $\beta_2$ -adrenergic agonist salbutamol potentiates oral induction of tolerance, suppressing adjuvant arthritis and antigen-specific immunity. *J. Immunol.* 169, 5028–5035
- 21 Kruszezwska, B. *et al.* (1995) Alterations in cytokine and antibody production following chemical sympathectomy in two strains of mice. *J. Immunol.* 155, 4613–4620
- 22 Wahle, M. *et al.* (1999) Disease activity related catecholamine response of lymphocytes from patients with rheumatoid arthritis. *Ann. N. Y. Acad. Sci.* 876, 287–296
- 23 Zoukos, Y. *et al.* (1992)  $\beta$ -Adrenergic receptor density and function of peripheral blood mononuclear cells are increased in multiple sclerosis: a regulatory role for cortisol and interleukin-1. *Ann. Neurol.* 31, 657–662
- 24 von Hörsten, S. *et al.* (2004) PP, PYY and NPY: synthesis, storage, release and degradation. In *Handbook of Pharmacology* (Vol. 162) (Michel, M., ed.), pp. 23–44, Springer Press
- 25 Bedoui, S. *et al.* (2002) NPY modulates epinephrine-induced leukocytosis via Y-1 and Y-5 receptor activation *in vivo*: sympathetic co-transmission during leukocyte mobilization. *J. Neuroimmunol.* 132, 25–33
- 26 Straub, R.H. *et al.* (2000) Neuropeptide Y cotransmission with norepinephrine in the sympathetic nerve-macrophage interplay. *J. Neurochem.* 75, 2464–2471
- 27 De la Fuente, M. *et al.* (1993) Stimulation of murine peritoneal macrophage functions by neuropeptide Y and peptide YY. Involvement of protein kinase C. *Immunology* 80, 259–265
- 28 Hernanz, A. *et al.* (2003) Effect of calcitonin gene-related peptide, neuropeptide Y, substance P, and vasoactive intestinal peptide on interleukin-1 $\beta$ , interleukin-6 and tumor necrosis factor- $\alpha$  production by peripheral whole blood cells from rheumatoid arthritis and osteoarthritis patients. *Regul. Pept.* 115, 19–24
- 29 Levite, M. *et al.* (1998) Neuropeptides, via specific receptors, regulate T cell adhesion to fibronectin. *J. Immunol.* 160, 993–1000
- 30 Kawamura, N. *et al.* (1998) Differential effects of neuropeptides on cytokine production by mouse helper T cell subsets. *Neuroimmunomodulation* 5, 9–15
- 31 Levite, M. (1998) Neuropeptides, by direct interaction with T cells, induce cytokine secretion and break the commitment to a distinct T helper phenotype. *Proc. Natl. Acad. Sci. U. S. A.* 95, 12544–12549
- 32 Maeda, K. *et al.* (1994) Cerebrospinal fluid (CSF) neuropeptide Y- and somatostatin-like immunoreactivities in man. *Neuropeptides* 27, 323–332
- 33 Bedoui, S. *et al.* (2003) Neuropeptide Y (NPY) suppresses experimental autoimmune encephalomyelitis: NPY1 receptor-specific inhibition of autoreactive Th1 responses *in vivo*. *J. Immunol.* 171, 3451–3458
- 34 Coppin, H. *et al.* (2004) A vulnerability locus to multiple sclerosis maps to 7p15 in a region syntenic to an EAE locus in the rat. *Genes Immun.* 5, 72–75
- 35 Holmlund, A. *et al.* (1991) Concentrations of neuropeptides substance P, neurokinin A, calcitonin gene-related peptide, neuropeptide Y and vasoactive intestinal polypeptide in synovial fluid of the human temporomandibular joint. A correlation with symptoms, signs and arthroscopic findings. *Int. J. Oral Maxillofac. Surg.* 20, 228–231
- 36 Reinhold, D. *et al.* (2002) The role of dipeptidyl peptidase IV (DP IV) enzymatic activity in T cell activation and autoimmunity. *Biol. Chem.* 383, 1133–1138
- 37 De Meester, I. *et al.* (1999) CD26, let it cut or cut it down. *Immunol. Today* 20, 367–375
- 38 Steinbrecher, A. *et al.* (2001) Targeting dipeptidyl peptidase IV (CD26) suppresses autoimmune encephalomyelitis and up-regulates TGF- $\beta$ 1 secretion *in vivo*. *J. Immunol.* 166, 2041–2048
- 39 Silva, A.P. *et al.* (2003) NPY, NPY receptors, and DPP IV activity are modulated by LPS, TNF- $\alpha$  and IFN- $\gamma$  in HUVEC. *Regul. Pept.* 116, 71–79
- 40 Walsh, D.A. and Haywood, L. (2001) Angiogenesis: a therapeutic target in arthritis. *Curr. Opin. Investig. Drugs* 2, 1054–1063

### Forthcoming conferences of interest

#### Neuroendocrine-Immune Interactions

Euroconference on Cytokines in the Brain: Expression and Action of Cytokines in the Brain and Pathophysiological Implications  
Giens (near Toulon), France – 8–13 October 2004  
<http://www.esf.org/euresco/04/mc04140>

#### 3rd International Conference on Innate Immunity

Crete, Greece – 10–15 October 2004  
<http://www.aegeanconferences.org/3rdInnate/>

#### 4th International Congress on Autoimmunity

Budapest, Hungary – 3–7 November 2004  
[www.kenes.com/autoim2004](http://www.kenes.com/autoim2004)

#### British Society for Immunology

Harrogate, UK – 7–10 December 2004  
<http://immunology.org/Congress/Progme.htm>

## PAPER

## Chronic inflammatory demyelinating polyneuropathy: decreased claudin-5 and relocated ZO-1

T Kanda, Y Numata, H Mizusawa

See end of article for authors' affiliations

*J Neural Neurosurg Psychiatry* 2004;75:765–769. doi: 10.1136/jnnp.2003.025692

Correspondence to:  
Dr T Kanda, Department of  
Neurology and  
Neurological Science,  
Tokyo Medical and Dental  
University Graduate  
School, 1-5-45 Yushima,  
Bunkyo-ku, Tokyo  
113-8519, Japan;  
t-kanda.nuro@tmd.ac.jp

Received 11 August 2003  
In revised form  
29 September 2003  
Accepted  
30 September 2003

**Objectives:** To clarify the dynamics of molecules composing the blood–nerve barrier (BNB) in inflammatory neuropathies.

**Methods:** The expression of four tight junction (TJ) proteins—claudin-1, claudin-5, occludin, and ZO-1—was analysed immunohistochemically in sural nerve biopsy specimens obtained from patients with chronic inflammatory demyelinating polyradiculoneuropathy (CIDP).

**Results:** Claudin-1 was detected only in perineurial cells, whereas claudin-5 was present in endothelial cells, irrespective of vessel location or size. Occludin and ZO-1 were found in perineurial cells, in addition to some epineurial and endoneurial endothelial cells. In CIDP, percentages of endoneurial small vessels immunoreactive for claudin-5 were significantly decreased, as were ZO-1 immunoreactive endoneurial small vessels, with staining localised to interfaces between cells. Claudin-1 and occludin immunoreactivity did not differ appreciably between the neuropathies examined.

**Conclusions:** The downregulation of claudin-5 and altered localisation of ZO-1 seen in CIDP specimens may indicate that BNB derangement occurs in inflammatory neuropathies. Further investigation of TJ molecules may suggest new treatments based on properties of the BNB.

Endothelial cells in the adult central nervous system (CNS) and also in the peripheral nervous system (PNS) are coupled by tight junctions (TJ) that resemble those of epithelial barriers<sup>1,2</sup> and show extremely low permeability. Breakdown of these TJs in the blood–nerve barrier (BNB) may allow antimyelin antibodies and various inflammatory cytokines to enter peripheral nerve tissues, exacerbating peripheral nerve injury in inflammatory neuropathies, including Guillain-Barré syndrome<sup>1</sup> and chronic inflammatory demyelinating polyneuropathy (CIDP). The development of new therapeutic strategies to restore BNB function based on the properties of TJs has long been awaited. Understanding of the molecular basis of TJs has been increasing since 1993, when occludin, a protein with four transmembrane domains, was discovered.<sup>3</sup> Occludin has also been detected in endothelial cells forming the blood–brain barrier (BBB).<sup>3</sup> Occludin deficient cells have been found to form morphologically normal TJs.<sup>4</sup> However, a new family of TJ proteins, claudins, has received attention more recently. Claudins also have four transmembrane domains, but do not show homology to occludin.<sup>5</sup> Among claudin family members, claudin-1, claudin-5, and claudin-11 have been demonstrated in the brain.<sup>7,8</sup> Because claudin-11 is expressed only in oligodendrocytes,<sup>7</sup> and presumably is not related to endothelial barriers, we focused on claudin-1 and claudin-5 as molecules of interest concerning the barrier system in both the CNS and PNS. In our present study, using immunohistochemistry, we analysed the expression of four representative TJ proteins—claudin-1, claudin-5, occludin, and ZO-1—in the human PNS using sural nerve biopsy specimens. We examined the expression of these molecules in PNS disorders in which BNB breakdown is believed to have an important pathogenetic role.

## MATERIALS AND METHODS

## Patients

Sural nerve biopsy specimens obtained from 25 patients including 10 from patients with CIDP (eight men and two

women; age range, 13–64 years; mean, 44.3) were studied. Informed consent was obtained from each patient. The study complied with the ethical guidelines of Tokyo Medical and Dental University. Diagnoses were based on detailed clinical and electrophysiological investigations of the patients, in addition to the pathological examination of sural nerve specimens, including toluidine blue stained semithin sections and teased fibre preparations. CIDP was diagnosed according to standard criteria,<sup>9</sup> and all 10 patients were categorised as “definite” CIDP. Table 1 lists the clinical features and immunostaining results in the patients with CIDP. Other nerve biopsy specimens studied as disease controls included those obtained from six patients with vasculitic neuropathy associated with the Churg-Strauss syndrome (three men and three women; age range, 44–67 years; mean, 57.2); six with hereditary neuropathy (three men and three women; age range, 17–61 years; mean, 45.5; five with type I Charcot-Marie tooth disease and one with hereditary sensory and autonomic neuropathy type II); and four with nutritional neuropathy resulting from vitamin B<sub>12</sub> deficiency (three men and one woman; age range, 23–62 years; mean, 45.8). Specimens were snap frozen and stored at –80°C until use.

## Immunohistochemical techniques

Rabbit polyclonal antibodies against human claudin-1, claudin-5, occludin, and ZO-1 were purchased from Zymed (South San Francisco, California, USA). Serial transverse sections (10 µm thick) were cut from specimens on a cryostat, fixed in acetone at 4°C for five minutes, and then exposed to 0.03% H<sub>2</sub>O<sub>2</sub>/methanol for 10 minutes at room temperature. Sections were then preincubated in phosphate buffered saline (PBS) supplemented with 10% normal goat serum for three hours before incubating overnight with

**Abbreviations:** BBB, blood–brain barrier; BMEC, brain microvascular endothelial cell; BNB, blood–nerve barrier; CNS, central nervous system; CIDP, chronic inflammatory demyelinating polyneuropathy; PBS, phosphate buffered saline; PNS, peripheral nervous system; TJ, tight junction; VEGF, vascular endothelial growth factor



**Table 1** Clinical features and immunostaining results in 10 patients with chronic inflammatory demyelinating polyradiculoneuropathy

Patient	Age/sex	Biopsy (months)	CSF protein (mg/l)	Symptoms	Course	Nerve conduction findings	Antiganglioside antibodies	Anti-C5+ microvessels (%)	ZO-1+ vessels positive at endothelial cell interfaces (%)
1	13 M	10	1170	Mo>Se	Progr	D	—	27.4	57.1
2	24 M	6	960	Mo=Se	Progr	D	—	70.9	11.1
3	31 M	3	1670	Mo=Se	Progr	D	—	38.4	40.0
4	32 F	4	880	Mo=Se	Progr	D+A	GM1 (IgM)	69.4	78.1
5	41 M	5	680	Mo=Se	RR	D	GM1, GD1b, SGPG	72.6	85.7
6	55 F	2	1140	Mo=Se	Progr	D	—	93.2	†
7	58 M	6	1100	Mo<Se	Progr	D	SGLPG	52.2	41.1
8	62 M	3	1610	Mo<Se	RR	D	—	94.5	13.3
9	63 M	72+	9520	Mo=Se	Progr	D	—	63.2	33.3
10	64 M	2	1850	Mo=Se	RR	D	SGLPG	24.3	55.6

\*Percentage of ZO-1 immunoreactive endoneurial vessels showing immunoreactivity at endothelial cell interfaces; †ZO-1 immunoreactivity was too faint for the percentage of vessels showing immunoreactivity at endothelial cell interfaces to be evaluated.

Age, age at the time of biopsy; Biopsy, months from disease onset to biopsy; CSF, cerebrospinal fluid; C5, claudin-5; Mo, motor symptoms; Se, sensory symptoms; Course, clinical course until biopsy; Progr, progressive; RR, relapsing and remitting; D, demyelinating; A, axonal; SGPG, sulfoglucuronosyl paragloboside; SGLPG, sulfoglucuronosyl lactosaminyl paragloboside.

primary antibody diluted in PBS. Anti-claudin-5 and anti-occludin antibodies were used at a 1/400 dilution, whereas others were used at a 1/800 dilution. Sections were then rinsed with PBS three times before incubation for one hour with peroxidase conjugated secondary antibody (Nichirei, Tokyo, Japan). The reaction product indicating immunoreactivity in sections was developed with diaminobenzidine.

#### Analysis of claudin-5 positive microvasculature

We analysed endoneurial microvessels less than 30 µm in diameter, which included capillaries and some precapillary arterioles and postcapillary venules. Vessels apparently surrounded by perineurial cell layers were excluded. Because microvessels in the endoneurium were difficult to count accurately in cryostat sections, whether haematoxylin and eosin stained or immunostained using endothelial markers, such as anti-von Willebrand antigen, we first counted these vessels using toluidine blue stained, plastic embedded semithin sections to evaluate the density of endoneurial microvessels/mm<sup>2</sup>. The percentage of claudin-5-positive endoneurial microvessels was calculated as the density of anti-claudin-5 immunoreactive microvessels in cryostat sections ×100/overall density of microvessels in toluidine blue stained sections. If the first density exceeded the last, the percentage of claudin-5 immunoreactive microvessels was considered to be 100%. More than 0.5 mm<sup>2</sup> surface area of endoneurial space was evaluated in each specimen.

#### Analysis of staining pattern by anti-ZO-1 antibody

The percentage of endoneurial microvessels showing ZO-1 immunoreactivity localised at interfaces between adjoining endothelial cells was evaluated. Microvessels showing two or more immunoreactive lines across the endothelial cell layer, or two or more immunoreactive dots located at the luminal side of endothelial cells (fig 1) were judged to have ZO-1 localised at these endothelial cell borders. The percentage of ZO-1 immunoreactive cells with this localisation pattern was calculated as the number of endoneurial microvessels showing linear or punctate ZO-1 immunoreactivity at borders between endothelial cells ×100/overall number of ZO-1 immunoreactive endoneurial microvessels.

## RESULTS

Claudin-1 immunoreactivity was evenly present in the perineurial cell layers, with no clear difference in immunoreactivity between the inner and outer layers. No specimen showed staining of endothelial cells (figs 2A and 3). No

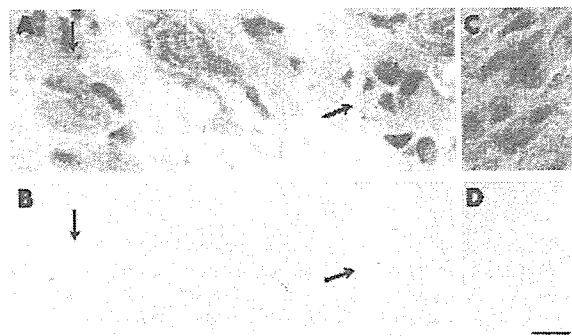


**Figure 1** Immunostaining with anti-ZO-1 antibody (B and D) and corresponding serial sections (A and C; haematoxylin and eosin staining) in sural nerves from a 67 year old woman with Churg-Strauss syndrome (A and B) and a 58 year old man with chronic inflammatory demyelinating polyneuropathy (CIPD) (C and D). ZO-1 immunoreactivity in endoneurial microvessels was localised to the interfaces between endothelial cells (arrows), especially at the luminal surface (note the punctate staining of the microvessel on the left in B). In CIPD, endothelial immunoreactivity was diffuse and weak (D); most strong staining localised to the intercellular borders had disappeared. Bar, 10 µm.

difference in claudin-1 immunoreactivity was noted between CIPD and the other disease groups (fig 3).

The polyclonal anti-occludin antibody stained the perineurial cell layers. In addition, the luminal aspect of some epineurial vessels and a small proportion of endoneurial capillaries adjacent to the perineurium was also immunoreactive (fig 2B). Endoneurial microvessels situated near the centre of the endoneurial space that were not neighbouring perineurial cell layers were not stained. No appreciable difference in immunoreactivity was noted between CIPD and the other disease groups.

Anti-ZO-1 immunoreactivity was localised to the perineurial cell layers, in addition to some endothelial cells lining epineurial vessels and the endoneurium (fig 2C). Although no detectable background staining was seen with the anti-occludin, anti-claudin-1, and anti-claudin-5 antibodies, faint background immunoreactivity was occasionally seen in the endoneurium with the anti-ZO-1 antibody. Therefore, the exact percentage of stained endoneurial microvessels was difficult to determine. Instead, we calculated the percentage of endoneurial microvessels showing immunoreactivity localised to the junctions between endothelial cells (fig 1). In CIPD specimens, the percentage of endoneurial microvessels

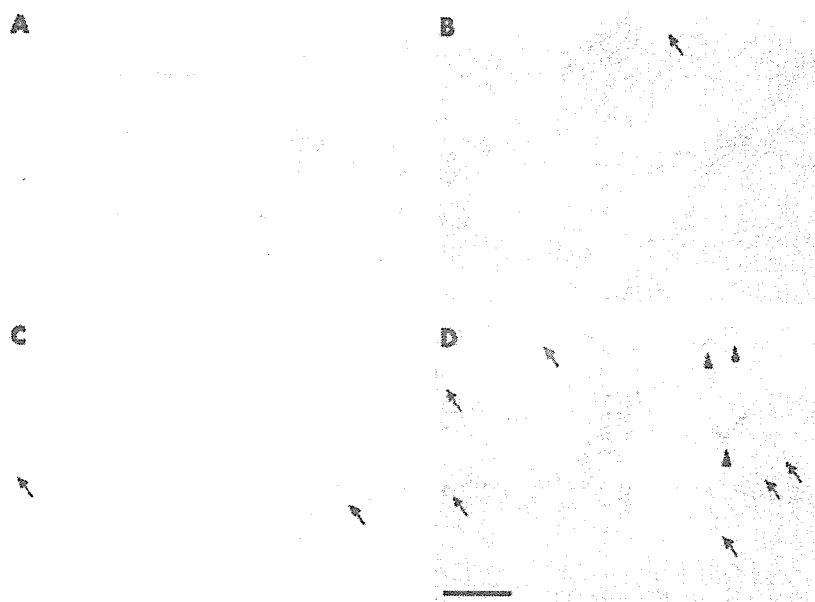


**Figure 2** Immunostaining in serial sections obtained from a 64 year old man with Churg-Strauss syndrome with (A) anti-claudin-1, (B) anti-occludin, (C) anti-ZO-1, and (D) anti-claudin-5 antibodies, showing a normal pattern of staining in the human peripheral nervous system. (A) Anti-claudin-1 antibody stained perineurial cell layers exclusively, with no immunoreactivity against endothelial cells. (B) Anti-occludin immunoreactivity was noted in perineurial cell layers. In addition, faint staining was seen in the endothelial cell layers of epineurial vessels (arrow). (C) The anti-ZO-1 antibody reacted faintly with epineurial cell layers and some of the endothelial cells in the endoneurium (arrows). (D) Unlike the other three antibodies, anti-claudin-5 antibody stained endothelial cells exclusively, irrespective of their vessel size or location. Endothelial cells in the epineurium (arrowheads) and in the endoneurium (arrows) were immunoreactive. Bar, 100  $\mu$ m.

with such anti-ZO-1 immunoreactivity localisation was significantly lower (fig 4).

Claudin-5 was detected exclusively in endothelial cells, irrespective of the location or size of the vessel in the control specimen (figs 2D and 5). Unlike anti-ZO-1 immunostaining, immunoreactivity was not detected at endothelial cell interfaces. In CIDP, the percentage of anti-claudin-5 immunoreactive microvessels in the endoneurium was significantly decreased compared with non-inflammatory neuropathies (figs 5 and 6). No apparent correlation was noted between the loss of claudin-5 immunoreactivity and endoneurial/subperineurial oedema

## DISCUSSION

In inflammatory neuropathies including CIDP, increases in cytokines such as interleukin  $1\beta$ ,<sup>11,12</sup> tumour necrosis factor  $\alpha$ ,<sup>11,12</sup> and vascular endothelial growth factor (VEGF)<sup>14</sup> are

believed to contribute to pathogenesis through modulation of the BNB. Among these, VEGF acts as a particularly potent disrupter of the BNB in various inflammatory neuropathies.<sup>14</sup> This increase in vascular permeability occurs through the binding of VEGF to its tyrosine kinase-type receptors, flt-1 and flt-k,<sup>15</sup> resulting in a decrease in TJ proteins, including occludin and vascular endothelial cadherin, and subsequent disorganisation of interendothelial cell junctions.<sup>16</sup> Thus, study of the molecular dynamics of TJ proteins in human inflammatory neuropathies may improve understanding of BNB derangement and prompt the development of new therapeutic approaches in these disorders. Recent experiments have indicated that the establishment of TJ strands depends on claudin family proteins. For example, the transfection of claudin-1 and claudin-2 into fibroblasts induces the formation of TJ strands.<sup>17</sup> Claudin-11 knockout

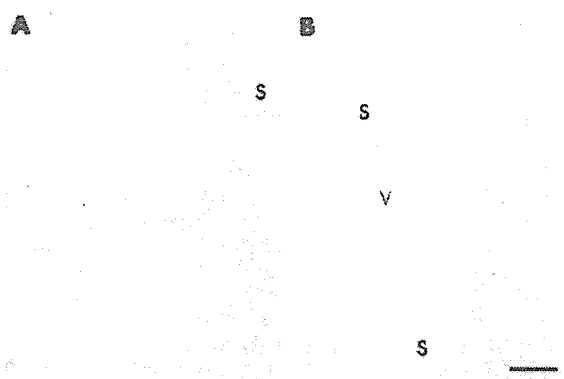


**Figure 3** Claudin-1 immunostaining in a control specimen from (A) a 67 year old woman with Churg-Strauss syndrome (CSS) and (B) a specimen from a 55 year old woman with chronic inflammatory demyelinating polyneuropathy (CIDP). Claudin-1 immunoreactivity was detected exclusively in the perineurial cell layers, and no endothelial staining was noted in the endoneurium or epineurium (V). Sections from CIDP and CSS were stained equally. V designates a medium sized epineurial vessel and S designates small sized nerve fascicles. Bar, 100  $\mu$ m.

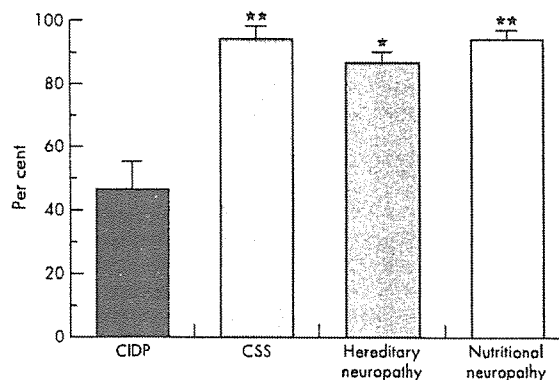


**Figure 4** Mean percentage of all ZO-1 immunoreactive endoneurial microvessels showing localisation of ZO-1 immunoreactivity to the interfaces between endothelial cells in specimens with chronic inflammatory demyelinating polyneuropathy (CIDP) (mean, 46.1%; SEM, 8.6%), Churg-Strauss syndrome (CSS) (mean, 93.8%; SEM, 3.7%), hereditary neuropathy (mean, 86.3%; SEM, 3.1%), and nutritional neuropathy (mean, 94.0%; SEM, 2.1%). CIDP specimens showed a significantly lower percentage of endoneurial microvessels with this localisation of ZO-1 immunoreactivity. \* $p < 0.005$  v CIDP; \*\* $p < 0.002$  v CIDP. Bars indicate SEM.

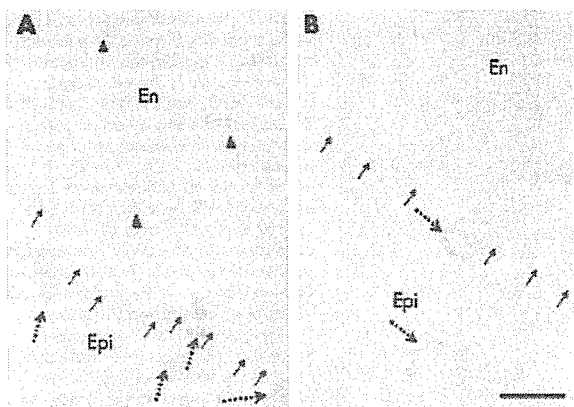


**Figure 5** Claudin-5 immunostaining in (A) a control specimen from a 67 year old woman with Churg-Strauss syndrome and (B) a 31 year old man with chronic inflammatory demyelinating polyneuropathy (CIDP). The small arrows indicate the outer aspect of the endoneurium. In the control (A), claudin-5 immunoreactivity was detected exclusively in endothelial cells, irrespective of vessel size or location. Dotted arrows indicate immunoreactive microvessels in the epineurium and arrowheads indicate those in the endoneurium. In CIDP (B), although medium sized vessels in the epineurium were well stained (dotted arrows), immunoreactivity in the endoneurium was severely decreased. En, endoneurium; Epi, epineurium. Bar, 50  $\mu$ m.

mice show absence of TJ strands in the myelin sheets of oligodendrocytes and Sertoli cells,<sup>18</sup> whereas claudin-16 knockout mice demonstrate abnormal paracellular passage of  $Mg^{2+}$  ions.<sup>19</sup> Accordingly, we first focused on the expression of two claudin family members, claudin-1 and claudin-5, in sural nerve biopsy specimens.

Claudin-5, which localises exclusively to borders between adjacent endothelial cells,<sup>20</sup> is considered to be important in the control of vascular permeability. Recently Nitta *et al* reported the selective leakage of small molecules (< 800 Da) across the BBB in claudin-5 deficient mice.<sup>21</sup> This suggests that claudin-5, although ubiquitously present in all endothelial cells, plays a special role in the barrier mechanism of the nervous system by preventing the entrance of such small molecules. In their article, no information was given about the BNB, but free entrance of small molecules through claudin-5 deficient endothelial junctions may also occur in the PNS. Hence, the loss of claudin-5 in the endoneurial microvessels in patients with CIDP may enhance the leakage of small molecules into the endoneurial space, and may result in changes to the endoneurial constituents that are unfavourable to Schwann cells and axons, eventually leading to the worsening of neuropathy. However, we found no correlation between the loss of claudin-5 immunoreactivity and the presence of endoneurial/subperineurial oedema; in addition, *Cld5*<sup>-/-</sup> mice do not show vasogenic oedema. This might be explained by the fact that even in claudin-5 deficiency most serum proteins (molecular mass > 800 Da) cannot extravasate.<sup>21</sup> Endoneurial/subperineurial oedema, a relatively common finding in sural nerve specimens from patients with CIDP,<sup>22</sup> may be elicited by factors other than a decrease in claudin-5 expression.

The disagreement between our BNB findings and previous observations concerning the BBB<sup>20</sup> is somewhat difficult to account for; one explanation is that downregulation of claudin-5 in endoneurial microvessels in CIDP might be a BNB specific phenomenon, reflecting differences in anatomic structure and cell populations (for example, the absence of astrocytes). Of 10 CIDP specimens, two (from patients 6 and 8) showed normal anti-claudin-5 immunoreactivity in

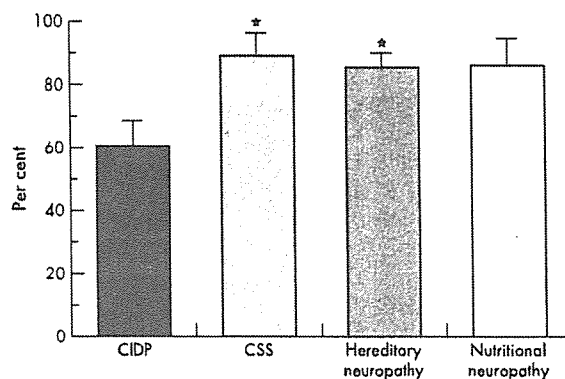


**Figure 6** Mean percentage of endoneurial microvessels immunoreactive with anti-claudin-5 antibody in specimens with chronic inflammatory demyelinating polyneuropathy (CIDP) (mean, 60.6%; SEM, 7.8%), Churg-Strauss syndrome (CSS) (mean, 89.5%; SEM, 6.5%), hereditary neuropathy (mean, 85.6%; SEM, 4.0%), and nutritional neuropathy (mean, 86.2%; SEM, 8.4%). Staining with the anti-claudin-5 antibody in the endothelial cells of the endoneurium was significantly decreased in CIDP specimens compared with CSS and hereditary neuropathy. \* $p < 0.05$  v CIDP. Bars indicate SEM.

endoneurial microvessels; this could reflect a non-uniform or multifocal, rather than diffuse, distribution of demyelination foci in this disorder.<sup>23</sup> However, these two specimens showed extremely faint ZO-1 immunoreactivity (patient 6) or a very low percentage of endoneurial vessels showing ZO-1 immunoreactivity at intercellular interfaces (patient 8). Thus, changes of expression of claudin-5 and ZO-1 are not always in parallel with CIDP, suggesting functional differences between these two TJ proteins.

Although claudin-1 is the only member of the claudin family (except for claudin-5) that might be expected to be present in endothelial cells, we found no staining for claudin-1 in the endothelial cells of the PNS. Instead, the anti-claudin-1 antibody exclusively stained the perineurial cell layers. Because the BNB includes the endoneurial microvasculature and the innermost layer of the perineurium,<sup>24-25</sup> anti-claudin-1 immunoreactivity might be taken to represent the latter. However, the uniform staining of all perineurial cell layers that was seen does not correspond well to the site of the BNB. In addition, claudin-1 immunoreactivity was almost as abundant in CIDP as in control specimens. Therefore, claudin-1 is not a marker of BNB integrity.

In our present study, we detected occludin immunoreactivity in endothelial cells of some epineurial vessels, a small percentage of endoneurial capillaries adjoining perineurial cell layers, and perineurial cells. However, we saw no appreciable differences in occludin immunoreactivity in the perineurial cell layer and in the endothelial cells between the various disorders. Occludin may not be essential for TJ formation,<sup>26</sup> but it has been reported to be abundant in relation to the endothelial cells of the brain, although it is undetectable in non-neural tissues.<sup>3,26</sup> VEGF treatment of brain microvascular endothelial cell (BMEC) monolayer cultures decreased detectable occludin and disrupted its continuous pericellular distribution.<sup>27</sup> Although these reports suggest that occludin may play some part in the maintenance of BNB integrity, our results indicated that occludin does not change appreciably in inflammatory neuropathies.

ZO-1, a 220 kDa TJ phosphoprotein, is a member of the membrane associated guanylate kinases localised to intercellular contacts.<sup>28</sup> ZO-1 binds various proteins, including claudins and occludin, and may act as a molecular scaffold bringing these TJ constituents together.<sup>29</sup> Therefore, ZO-1 is expected to be a key molecule in the control of BNB integrity.

despite some previous conclusions that the expression and localisation of ZO-1 do not correlate with the physiological efficiency of paracellular barrier function.<sup>10</sup> In CIDP specimens, we found no significant decrease in ZO-1 immunoreactive endoneurial microvessels, although we noted a change in the staining pattern. This corresponds well with a recent observation that VEGF, known to open the BBB and BNB,<sup>14</sup> caused a loss of ZO-1 from endothelial cell junctions and changed the staining pattern at the cell boundary without decreasing ZO-1 content in cultured bovine BMEC.<sup>27</sup> We suspect that the change in the localisation of ZO-1 in CIDP specimens was an effect of various cytokines, including VEGF, that are upregulated in inflammatory neuropathies such as CIDP. The contribution of other inflammatory cytokines in addition to VEGF requires future investigation.

#### Authors' affiliations

T Kanda, Y Numata, H Mizusawa, Department of Neurology and Neurological Science, Tokyo Medical and Dental University Graduate School, 1-5-45 Yushima, Bunkyo-ku, Tokyo 113-8519, Japan

Competing interest: none declared

#### REFERENCES

- 1 Reese TJ, Karnovsky MJ. Fine structural localization of a blood-brain barrier to exogenous peroxidases. *J Cell Biol* 1967;34:207-17.
- 2 Rubin LL. Endothelial cells: adhesion and tight junction. *Curr Opin Cell Biol* 1992;4:830-3.
- 3 Kanda T, Yamawaki M, Mizusawa H. Sera from Guillain-Barré patients enhance leakage in blood-nerve barrier model. *Neurology* 2003;60:301-6.
- 4 Furuse M, Hirase T, Itoh M, et al. Occludin: a novel integral membrane protein localizing at tight junctions. *J Cell Biol* 1993;123:1777-88.
- 5 Hirase T, Staddon JM, Saitou M, et al. Occludin as a possible determinant of tight junction permeability in endothelial cells. *J Cell Sci* 1997;110:1603-13.
- 6 Saitou M, Fujimoto K, Dai Y, et al. Occludin-deficient embryonic stem cells can differentiate into polarized epithelial cells bearing tight junctions. *J Cell Biol* 1998;141:397-408.
- 7 Furuse M, Fujita K, Hiragaki T, et al. Claudin-1 and -2: novel integral membrane proteins localizing at tight junctions with no sequence similarity to occludin. *J Cell Biol* 1998;141:1539-50.
- 8 Morita K, Furuse M, Fujimoto K, et al. Claudin multigene family encoding four-transmembrane domain protein components of tight junction strands. *Proc Natl Acad Sci U S A* 1999;96:511-16.
- 9 Morita K, Sasaki H, Fujimoto K, et al. Claudin-11/OSP-based tight junctions of myelin sheaths in brain and Sertoli cells in testis. *J Cell Biol* 1999;145:579-88.
- 10 Research criteria for diagnosis of chronic inflammatory demyelinating polyneuropathy (CIDP). Report from an ad hoc subcommittee of the American Academy of Neurology AIDS Task Force. *Neurology* 1991;32:958-64.
- 11 Sharief MK, Ingram DA, Swash M. Circulating tumor necrosis factor- $\alpha$  correlates with electrodiagnostic abnormalities in Guillain-Barré syndrome. *Ann Neurol* 1997;42:68-73.
- 12 Zhu J, Bai XF, Mix E, et al. Experimental allergic neuritis: cytolytic mRNA expression is upregulated in lymph node cells during convalescence. *J Neuroimmunol* 1997;78:108-16.
- 13 Watanabe O, Arimura K, Kitajima I, et al. Greatly raised vascular endothelial growth factor (VEGF) in POEMS syndrome. *Lancet* 1996;347:702.
- 14 Kanda T, Iwasaki T, Yamawaki M, et al. Anti-GM1 antibody facilitates leakage in an in vitro blood-nerve barrier model. *Neurology* 2000;55:585-7.
- 15 Gale NW, Yancopoulos GD. Growth factors acting via endothelial cell-specific receptor tyrosine kinases: VEGFs, angiopoietins, and ephrins in vascular development. *Genes Dev* 1999;13:1055-66.
- 16 Kevil CG, Payne DK, Mire E, et al. Vascular permeability factor/vascular endothelial cell growth factor-mediated permeability occurs through disorganization of endothelial junctional proteins. *J Biol Chem* 1998;273:15099-103.
- 17 Tsulata S, Furuse M. Pores in the wall: claudins constitute tight junction strands containing aqueous pores. *J Cell Biol* 2000;149:13-16.
- 18 Gow A, Southwood CM, Li JS, et al. CNS myelin and Sertoli cell tight junction strands are absent in *Osp/claudin-11* null mice. *Cell* 1999;99:649-59.
- 19 Simon DB, Lu Y, Choate KA, et al. Paracellin-1, a renal tight junction protein required for paracellular  $Mg^{2+}$  resorption. *Science* 1999;285:103-6.
- 20 Morita K, Sasaki H, Furuse M, et al. Endothelial claudin: claudin-5/TMVCF constitutes tight junction strands in endothelial cells. *J Cell Biol* 1999;147:185-94.
- 21 Niita T, Hata M, Gotoh S, et al. Size-selective loosening of the blood-brain barrier in claudin-5 deficient mice. *J Cell Biol* 2003;161:653-60.
- 22 Kanda T, Yamawaki M, Iwasaki T, et al. Glycosphingolipid antibodies and blood-nerve barrier in autoimmune demyelinating neuropathy. *Neurology* 2000;54:1459-64.
- 23 Lewis RA, Sumner AJ. Electrophysiologic features of inherited demyelinating neuropathies: a reappraisal. *Ann N Y Acad Sci* 1999;883:321-5.
- 24 Bell MA, Weddell AGM. A descriptive study of the blood vessels of the sciatic nerve in the rat, man, and other mammals. *Brain* 1984;107:871-98.
- 25 Latker CH, Wadhvani KC, Baldo A, et al. Blood-nerve barrier in the frog during Wallerian degeneration: are axons necessary for maintenance of barrier function? *J Comp Neurol* 1991;309:650-64.
- 26 Saitou M, Ando-Akatsuka Y, Itoh M, et al. Mammalian occludin in epithelial cells: its expression and subcellular distribution. *Eur J Cell Biol* 1997;73:222-31.
- 27 Wang W, Denker WL, Borchardt RT. VEGF increases BMEC monolayer permeability by affecting occludin expression and tight junction assembly. *Am J Physiol* 2001;280:H434-40.
- 28 Mitic LL, Anderson JM. Molecular architecture of tight junctions. *Annu Rev Physiol* 1998;60:121-42.
- 29 Zahraoui A, Louvard D, Galli T. Tight junction, a platform for trafficking and signaling protein complexes. *J Cell Biol* 2000;151:F31-6.
- 30 Stevenson BR, Anderson JM, Goodenough DA, et al. Tight junction structure and ZO-1 content are identical in two strains of Madin-Darby canine kidney cells which differ in transepithelial resistance. *J Cell Biol* 1988;107:2401-8.